Am J Transl Res 2022;14(6):3658-3682
www.ajtr.org /ISSN:1943-8141/AJTR0141298

Original Article

Screening a novel six critical gene-based system of diagnostic and prognostic biomarkers in prostate adenocarcinoma patients with different clinical variables

Hadia Munir[1], Fawad Ahmad[2], Sajid Ullah[3], Saeedah Musaed Almutairi[4], Samra Asghar[5], Tehmina Siddique[6], Mostafa A Abdel-Maksoud[4], Rabab Ahmed Rasheed[7], Fatma Alzahraa A Elkhamisy[8,9], Mohammed Aufy[10], Hamid Yaz[4]

[1]Akhtar Saeed Medical and Dental College, Pakistan; [2]Rural Health Center Manthar, Rahim Yar Khan, Pakistan; [3]Cardiac ICU Medikay Cardiac Center Park Road Islamabad, Islamabad 4400, Pakistan; [4]Department of Botany and Microbiology, College of Science, King Saud University, Riyadh, P.O. 2455, Riyadh 11451, Saudi Arabia; [5]Department of Medical Laboratory Technology, Faculty of Rehablitation and Allied Health Sciences, Riphah International University, Faisalabad, Faisalabad, Pakistan; [6]Department of Biotechnology, Faculty of Life Sciences, University of Okara, Okara, Pakistan; [7]Histology and Cell Biology Department, Faculty of Medicine, King Salman International University, South Sinai, Egypt; [8]Pathology Department, Faculty of Medicine, Helwan University, Cairo, Egypt; [9]Basic Medical Sciences Department, Faculty of Medicine, King Salman International University, South Sinai, Egypt; [10]Department of Pharmaceutical Sciences, Division of Pharmacology and Toxicology, University of Vienna, Vienna, Austria

Received December 23, 2021; Accepted April 10, 2022; Epub June 15, 2022; Published June 30, 2022

Abstract: The mechanisms behind prostate adenocarcinoma (PRAD) pathogenicity remain to be understood due to tumor heterogeneity. In the current study, we identified by microarray technology six eligible real hub genes from already identified hub genes through a systematic *in silico* approach that could be useful to lower the heterogenetic-specific barriers in PRAD patients for diagnosis, prognosis, and treatment. For this purpose, microarray technology-based, already-identified PRAD-associated hub genes were initially explored through extensive literature mining; then, a protein-protein interaction (PPI) network construction of those hub genes and its analysis helped us to identify six most critical genes (real hub genes). Various online available expression databases were then used to explore the tumor driving, diagnostic, and prognostic roles of real hub genes in PRAD patients with different clinicopathologic variables. In total, 124 hub genes were extracted from the literature, and among those genes, six, including CDC20, HMMR, AURKA, CDK1, ASF1B, and CCNB1 were identified as real hub genes by the degree method. Further expression analysis revealed the significant up-regulation of real hub genes in PRAD patients of different races, age groups, and nodal metastasis status relative to controls. Moreover, through correlational analyses, different valuable correlations between treal hub genes expression and different other data (promoter methylation status, genetic alterations, overall survival (OS), tumor purity, CD4+ T, CD8+ T immune cells infiltration, and different other mutant genes and a few more) across PRAD samples were also documented. Ultimately, from this study, a few important transcription factors (TFS), miRNAs, and chemotherapeutic drugs showing a great therapeutic potential were also identified. In conclusion, we have discovered a set of six real hub genes that might be utilized as new biomarkers for lowering heterogenetic-specific barriers in PRAD patients for diagnosis, prognosis, and treatment.

Keywords: PRAD, tissue microarray, biomarker, overall survival (OS), heterogeneity

Introduction

Prostate adenocarcinoma (PRAD) is one of the prevalent tumors of the urogenital tract worldwide, accounting for nearly 1.4 million new cancer cases and 376,000 cancer-related deaths in year 2020 [1]. Different risk factors such as age, family history, environmental stress, occupational hazard, chemicals, radiation, and dietary components have been reported to be involved in PRAD development, but the studies lack precise mechanistic detail [2, 3]. Moreover, androgens, certain hormones, epithelial cells, and tumor microenvironment have also

been regarded as key players of PRAD development and progression [4, 5].

Nowadays, PRAD diagnosis is a challenging task due to the lack of highly specific biomarkers [6]. Currently, the most extensively utilized biomarker for PRAD diagnosis is prostate-specific antigen (PSA) [7], which has limited specificity and sensitivity [8], as it leads to over-diagnosis at the rate of 1.7-67% [9]. Additionally, several serum-based biomarkers expressed in the prostate epithelium have also been used to diagnose PRAD including Prostate Acid Phosphatase (PAP) [10], Prostate-Specific Membrane Antigen (PSMA) [11], Prostate Stem Cell Antigen (PSCA) [12], and Prostate Cancer gene 3 (PCA3) [13]; however, none of these biomarkers is ideal.

In the past decade, researchers have widely used next-generation sequencing (NGS) and microarray techniques to discover new biomarkers and therapeutic targets of PRAD [14]. However, the small sample size in individual studies has created substantial inter-study variability. In order to address this issue, worldwide available datasets on PRAD expression have been submitted to the Gene Expression Omnibus (GEO) database [15] by researchers so that these datasets can be integrated further using diverse methodologies to discover biomarkers as hub genes. Previous studies have integrated different PRAD GEO expression datasets to discover PRAD-associated hub genes as biomarkers [14, 16, 17]; however, keeping in view the fact that biomarkers are highly race, age, and nodal metastasis status-specific biomolecules, and knowing that GEO-based PRAD microarray expression datasets belong to PRAD patients of diverse attributes including different races, ages, and nodal metastasis status, it is clinically impossible to use already-identified GEO-based biomarkers in PRAD patients with different clinical variables over the heterogeneity-specific barriers.

Therefore, based on already-reported biomarkers (hub genes) from GEO microarray expression datasets of PRAD, it is necessary to discover a system of some diagnostic and prognostic biomarkers that could commonly be employed in PRAD patients with different clinical variables over the heterogeneity-specific barriers for better management of cancer.

In this study, six hub genes including CDC20, HMMR, AURKA, CDK1, ASF1B, and CDC20, were explored and validated as novel biomarkers of PRAD patients across the race, age, and nodal metastasis status heterogeneity-specific barriers through an *in silico* approach.

Materials and methods

Hub gene extraction by literature mining

We carried out a PubMed-based search to explore research articles that analyzed PRAD GEO microarray datasets to identify hub genes until August 2021. Two keywords used for search purpose were “Hub genes AND Prostate cancer/adenocarcinoma” and “Hub genes AND Prostate neoplasia”. Moreover, to refine the search, an “Original article” filter was also employed during the search process. At the completion of search process, a total of 222 original articles appeared, out of which only 17 articles were selected for further data extraction which collectively used 35 GEO PRAD microarray datasets and identified numerous hub genes. After selecting the articles, we manually extracted and combined all the identified hub genes reported in these articles to make a consolidated pool.

Real hub gene exploration by protein-protein interaction network, and their enrichment analysis

STRING database (http://www.stringdb.org/) [18] was herein used to construct a PPI network of pooled hub genes. Then, the constructed PPI network was analyzed by Cytoscape (v.3.51) [19], which helped us to identify the most significant module and real hub genes in the PPI network using MCODE and Cytohubba applications. Ultimately, the DAVID tool was employed to explore the real hub genes-related Gene Ontology (GO) and Kyoto Encyclopedia of Genes and Genomes (KEGG) terms. A p-value of <0.05 was set as the filter criterion.

Real-hub genes-related mRNA expression level variations

In this study, A UALCAN [20] based TCGA PRAD dataset consisting of 497 cancerous and 52 normal samples was used to analyze the expression variations in the real hub gene expression. For statistics, a t-test was employed and gene expression data were normalized as transcript per million (TPM) reads. A p-value <0.05 was considered significant.

Transcription and translation expression validation of real hub genes by TIMER, GENT2, GEPIA, DriverDBV3, and human protein atlas (HPA) dataset analysis

The TIMER (http://timer.cistrome.org/) [21], GENT2 (http://gent2.appex.kr/gent2/) [22], GEPIA (http://gepia.cancer-pku.cn/), DriverDBV3 (http://driverdb.tms.cmu.edu.tw/) [23], and HPA (https://www.proteinatlas.org/) [24] are the publicly available tools specialized in the TCGA or published cancer-related multi-omics data mining and analysis [21]. In this study, we utilized TIMER, GENT2, GEPIA, and DriverDBV3 tools for the mRNA expression validation, while using HPA for the translational expression validation of the real hub genes using new independent cohorts of PRAD patients. In addition, we also used one of these tools, UALCAN to validate the expression of real hub genes in PRAD patients of different races, ages, and nodal metastasis status. For statistics, TIMER, GENT2, GEPIA, and DriverDBV3 used a Student t-test and normalized the obtained mRNA expression as transcript per million (TPM) reads, while in HPA, translational expression is measured based on antibody-based images and mass spectrometry-based proteomics. A p-value <0.05 was considered significant.

Exploring correlation among real hub gene expression and their promoter methylation levels

MEXPRESS (https://mexpress.be/) [25] database was used here in the study to explore correlations among real hub gene expression and their promoter methylation levels across PRAD through Pearson correlation analysis. A p-value <0.05 was considered significant.

Effect of real hub genes dysregulation on the survival of PRAD patients

Kaplan-Meier Plotter (KM Plotter, http://kmplot.com/analysis/) repository has the capacity to store and retrieve huge amounts of data based on measuring the impact of 54k genes on the survival duration of more than 20 types of cancer patients [26]. Herein, we used this tool to analyze the effect of real hub genes on the Overall Survival (OS) of PRAD patients. A p-value <0.05 was considered significant.

cBioPortal

cBioPortal database (http://www.cbioportal.org) [27] was utilized in this study to explore genomic alteration and mutational hotspots in real hub genes across PRAD samples.

TIMER database

Using TIMER database (https://cistrome.shinyapps.io/timer/) [28] we explored the associations among tumor purity, CD4+ T, CD8+ T immune cells infiltration, and the mRNA expression level of real hub genes across PRAD samples. A p-value <0.05 was considered significant.

TF-miRNA-mRNA network

TF-miRNA-mRNA network related to real hub genes was constructed using ENCORI (http://starbase.sysu.edu.cn/) databases [29]. Moreover, Cytoscape (3.8.2) was further used to visualize and analyze the interaction network between targeted TFs, miRNAs, and real hub genes mRNA.

dbDEMC analysis

The dbDEMC database (http://www.picb.ac.cn/dbDEMC/index.html) [30] is dedicated to miRNAs expression profiling across multiple human cancers. The expression profiling of miRNAs targeting real hub genes in PRAD was done using the dbDEMC database.

CancerSEA analysis

CancerSEA (http://biocc.hrbmu.edu.cn/CancerSEA/) is developed for decoding Pearson correlation between gene(s) of interest and 14 different functional states at a single-cell level in human cancers [31]. Herein, we utilized CancerSEA to explore the correlation between real hub genes and the above-mentioned functional states in PRAD. A p-value <0.05 was considered significant.

MuTarget analysis

The MuTarget (https://www.mutarget.com/) is an online platform which associates gene expression alterations with mutational status in human cancers [32]. In our study, we used this platform to identify the mutant genes responsible for the expression alteration in the real hub genes across PRAD samples. A p-value <0.05 was considered significant.

Novel drugs prediction for real hub genes

Comparative toxicogenomics database (CTD, http://ctdbase.org/) [33], which in-house the

Table 1. List of the PRAD microarray expression datasets and the hub genes extracted selected studies

Dataset	No. samples C/N	Source of origin	Extracted hub genes	References
GSE6919	232/272	USA	RRM2, KIFC1, TACC3, PRC1, BIRC5, CDK1, ASF1B, E2F1, RACGAP1, MYBL2, TPX2, CDC20, TOP2A, NUSAP1, UBE2T, LMNB1, CCNB1, ZWINT, STMN1, TK1, CDH1, BMP2, NKX3-1, PPARG, PRKAR2B, EGFR, VEGFA, PIK3R1, DLG4, TGFBR1, KIT, HSPA8, PPP2R1A, CTNNB1, ADCY5, ANXA1, COL9A2, EPCAM, TWIST1, CD38, TCF3, MYC, MAX, CYP26A1, SREBF1, IFITM1, RTP4, ACSF2, GSTM2, GSTM1, ACOX2, COL4A6, ITGA2, AKR1B1, NPY, CFTR, GPX7, ALDH3A1, CRYZ, ALDH2, MAOB, GSTP1, GPX3, XAF1, BST2, FABP4, IGFBP3, THBS1, GJA1, UBE2C, KIF20A, PTTG1, TPM1, TAGLN, LMOD1, MYLK, ACTA2, TPM2, ACTG2, MYH11, MYL9, CALD1, IGF1, CD44, ITGB4, BCL2, LPAR3, LPAR1, TTK, CNN1, PBK, RAP1A, GNAS, RAB39B, COPZ2, KLF4, BACE1, COL12A1, ALB, ACACB, KLK3, IL10, ALDH1A3, KLK2, ALDH3B2, HBA1, COL1A1, NMU, GAL, F2RL1, PTGFR, AR, CXCR7, CCR7, NDRG1, NK3, CCNB2, CKS2, HMMR, CDKN3, AURKA, SPP1, FOS, and FOXA1	[109-125]
GSE6956	15/75	Maryland		
GSE32448	0/40	Maryland		
GSE32571	39/49	Germany		
GSE35988	28/59	USA		
GSE46602	0/50	Denmark		
GSE68555	181/263	USA		
GSE69223	15/15	Germany		
GSE70768	82/117	UK		
GSE88808	0/98	USA		
GSE26910	12/12	Italy		
GSE64318	28/26	USA		
GSE55945	8/13	USA		
GSE60329	27/109	Italy		
GSE103512	7/60	USA		
GSE45016	1/10	Japan		
GSE104749	4/4	China		
GSE55323	0/40	USA		
GSE26245	0/96	USA		
GSE26247	41/70	USA		
GSE65061	0/43	USA		
GSE62610	14/22	Denmark		
GSE46738	18/18	France		
GSE112047	16/31	Canada		
GSE76938	63/73	USA		
GSE7930	0/6	USA		
GSE6605	0/75	USA		
GSE6606	0/196	USA		
GSE26022	41/29	USA		
GSE30521	0/23	China		
GSE3325	6/13	USA		
GSE104935	0/10	USA		
GSE64143	0/2	USA		
GSE120005	0/3	USA		
GSE32269	4/51	USA		
Total = 35	Total = 882/2073		Total = 124	

information of relations between chemicals, genes of interest and diseases is used in this study to predict the novel drugs associated with real hub genes.

Results

Hub gene extraction through literature mining

In total, 17 articles were shortlisted which dealt with GEO PRAD microarray datasets and searched numerous hub genes. These studies were further explored to extract the hub genes in these studies and construct a pool after normalizing the duplicated genes. Ultimately, we were able to get a consolidated pool of 124 hub genes from 35 GEO microarray datasets consisting of 882 PRAD and 2073 normal samples (**Table 1**). The original data without normalization can be found in the Supplementary Table 1.

Real hub gene exploration from protein-protein interaction network, and their enrichment analysis

A STRING-based PPI network of pooled hub genes was obtained initially (**Figure 1A**). After that, MCODE and the Cytohubba application (via degree method) of Cytoscape were potentially used to analyze the significant module and identify the top six PRAD-linked genes (real hub genes). The identified module was consisted of 33 hub genes (**Figure 2B**, **2C**), and via degree method the identified real six hub genes were included CDC20, HMMR, AURKA, CDK1, ASF1B, and CCNB1 (**Figure 1C** and **Table 2**). Moreover, GO and KEGG enrichment analysis revealed the involvement of real hub genes in different GO and KEGG terms including G2/M transition of mitotic cell cycle, etc., BP terms, Centrosome etc. CC terms, Histone kinase activity etc. MF terms (**Figure 2** and **Table 3**), and Oocyte meiosis etc. KEGG terms (**Figure 2D** and **Table 4**).

Real hub gene expression analysis and validation

Expression analysis and validation of real hub gene expression (at mRNA and protein levels) across controls and cancerous samples of PRAD patients with different clinicopathologic variables including different races, ages, and nodal metastasis status was carried out through six different reliable platforms including UALCAN, TIMER, GENT2, GEPIA, DriverDBV2, HPA database. In view of the results of mRNA and protein expression analysis and validation using six different platforms including UALCAN, TIMER, GENT2, GEPIA, DriverDBV3, and HPA, it was observed that real hub genes (CDC20, HMMR, AURKA, CDK1, ASF1B, and CCNB1) were significantly ($P<0.05$) overexpressed at both mRNA and protein levels in PRAD patients of different race, age group, and nodal metastasis status as compared to controls (**Figures 3**-**5**).

Promoter methylation analysis of real hub genes in PRAD relative to controls

Associations between the promoter methylation and expression of real hub genes across PRAD samples relative to controls were analyzed by MEXPRESS. Results of the analysis revealed that all real hub genes including CDC20, HMMR, AURKA, CDK1, ASF1B, and CCNB1 were found notably hypomethylated relative to controls (**Figure 6**).

Prognostic significance of real hub genes

Prognostic significance of real hub genes in estimating the OS of PRAD patients was analyzed using KM plotter. In view of the analysis results, higher expressions of CDC20, HMMR, AURKA, CDK1, ASF1B, and CCNB1 were found to be significantly ($P<0.05$) associated with reduced OS of the PRAD patients (**Figure 7**). Therefore, it is speculated that those real hub genes could be potential prognostic biomarkers of PRAD patients for predicting their OS outcomes.

Real hub genes-associated genomic alterations

Six real hub gene-associated genomic alteration information was taken from three TCGA PRAD datasets including: Prostate Adenocarcinoma (MSKCC/DFCI, Nature Genetics 2018), Prostate Adenocarcinoma (TCGA Firehose Legacy), and Prostate Adenocarcinoma (TCGA PanCancer Atlas), available through cBioPortal platform. In view of our results, varying degrees of genetic variation were observed in real hub genes across PRAD samples. Out of all real hub genes, CCNB1 had shown the highest incidence rate (5%) of genetic variations followed by CDK1, which has shown the second highest genetic variations rate (2.9%). Other real hub genes, including HMMR, AURKA, CDC20, and ASF1B have shown genetic variations rates of 2%, 1.2%, 1%, and 0.4% in PRAD samples, respectively. Moreover, in all six real hub genes, the most frequently observed genetic alteration was deep amplification (**Figure 8A**). In addition, we further observed that the most frequent mutation in the CDC20 gene (W317*) was located in WD40 domain (**Figure 8B**). Similarly, in AURKA, the most frequently observed mutation (R220G) was present in the Pkinase domain (**Figure 8B**), while no mutations were detected in ASF1B and CCNB1. However, on the other hand, mutations in HMMR were found outside any functional domain (**Figure 8B**).

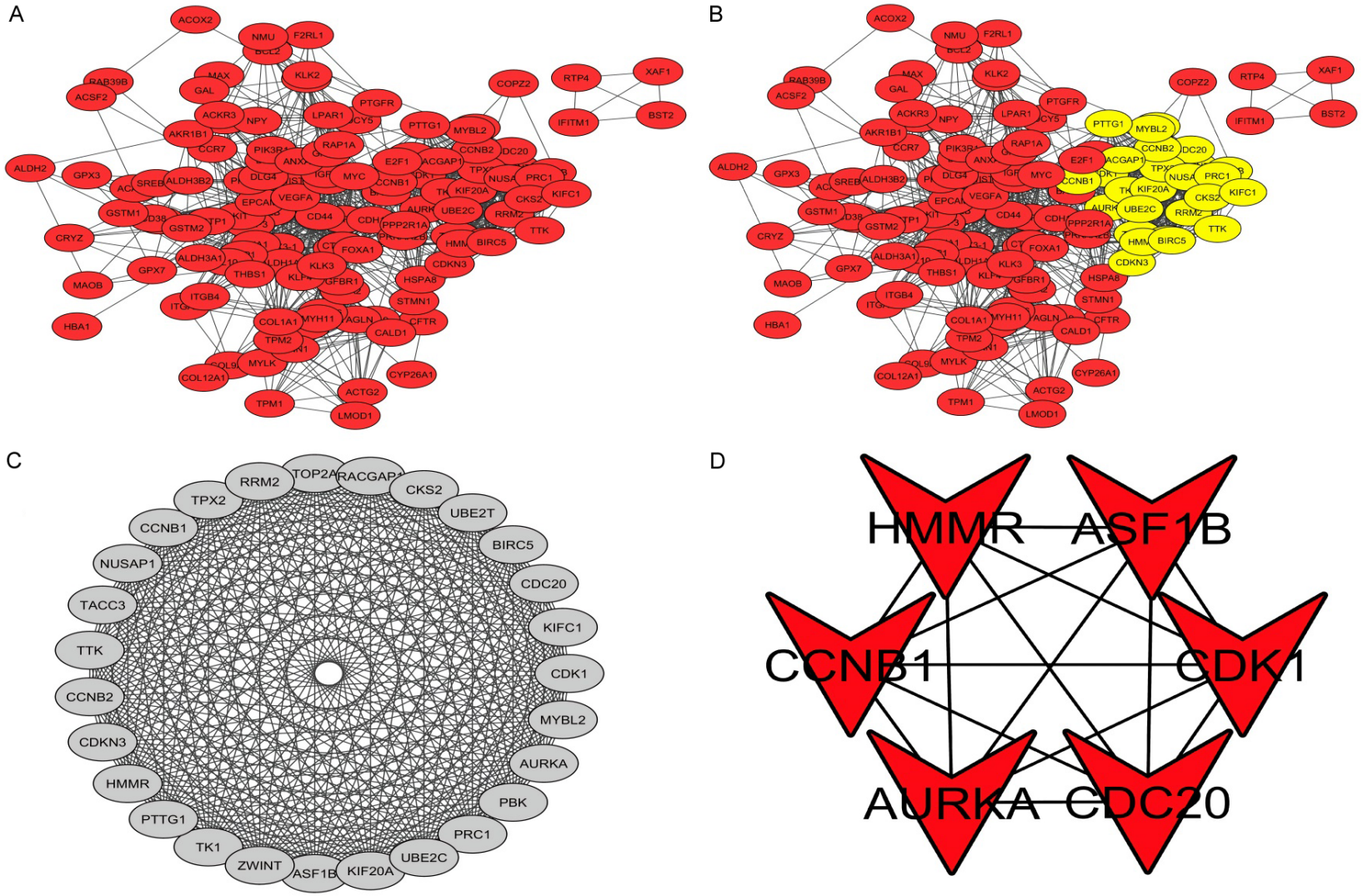

Figure 1. A PPI network construction and exploration of real hub genes. (A) A PPI network of extracted hub genes, (B) A significant module inside the PPI network, (C) Hub genes inside the significant module, and (D) Six identified real hub genes.

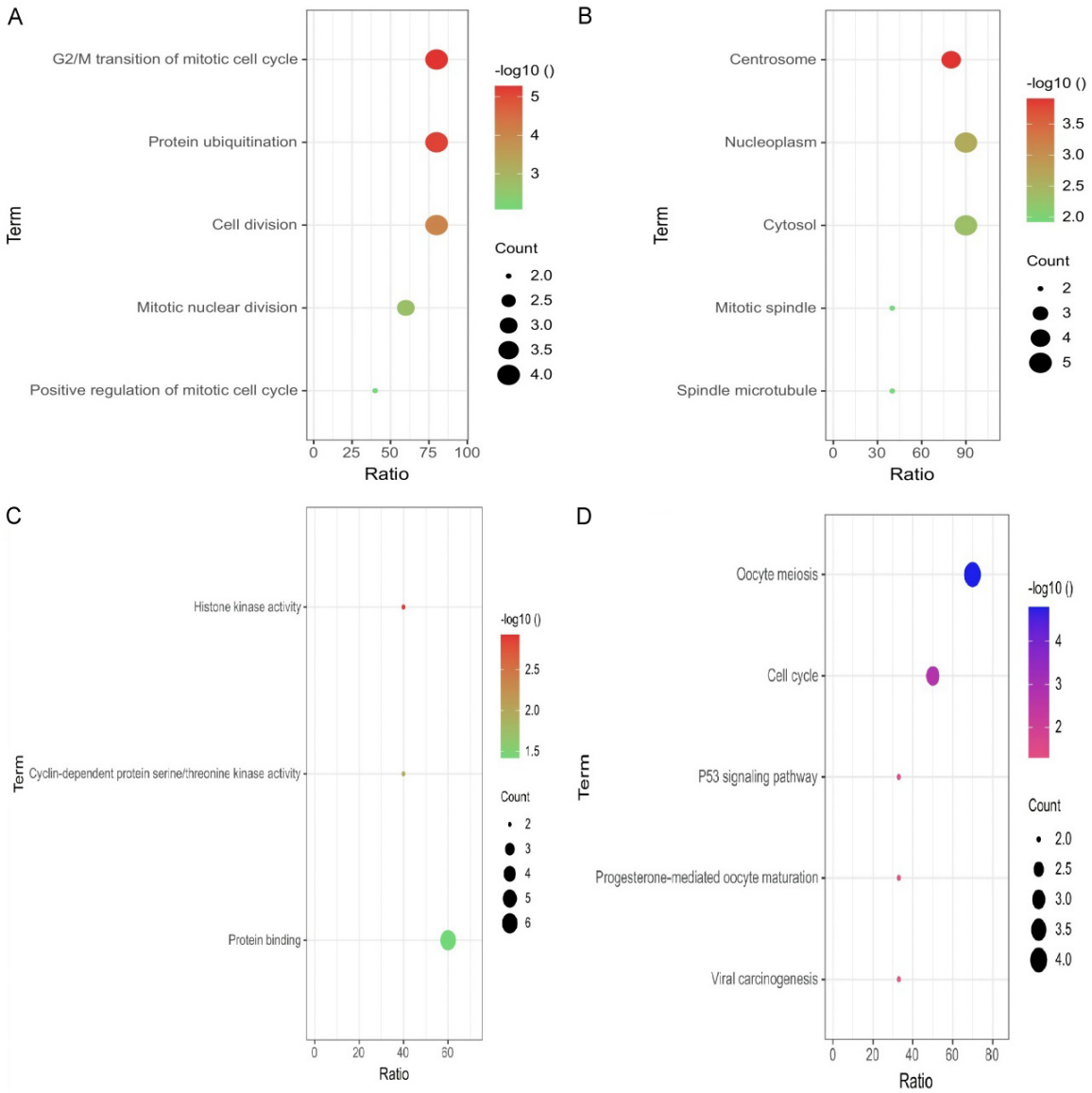

Figure 2. Enrichment (GO and KEGG) of real hub genes. (A) BF enrichment, (B) CC enrichment, (C) MF enrichment, and (D) KEGG enrichment. A *p*-value <0.05 was considered significant.

Table 2. List of the real hub genes identified from a PPI network of the extracted 124 PRAD related hub genes

Sr. No	Name of the gene	MCODE Node Status	MCODE Score
1	CDC20	Clustered	22.78769
2	HMMR	Clustered	22.78769
3	AURKA	Clustered	22.78769
4	CDK1	Clustered	22.78769
5	ASF1B	Clustered	22.78769
6	CCNB1	Clustered	22.78769

Immune cells infiltration analysis of real hub genes

By Spearman correlation analysis through the TIMER database, we observed notable positive correlations between real hub genes expression, tumor purity, and CD4+ T immune cells infiltration levels across PRAD samples (**Figure 9**). In addition, this analysis also showed a negative correlation between real hub genes expression and CD8+ T immune cells infiltration level across PRAD samples.

Table 3. Details of the GO analysis of identified hub genes extracted from various GEO PRAD expression microarray datasets

GO Term	GO ID	Gene count	*P*-value	Gene name
BP				
GO:0000086	G2/M transition of mitotic cell cycle	4	5.249880697116876E-6	CCNB1, CDK1, HMMR, AURKA
GO:0042787	Protein ubiquitination	4	7.3188630105038734E-6	CDC20, CCNB1, CDK1, AURKA
GO:0051301	Cell division	4	8.703225761335279E-5	CDC20, CCNB1, CDK1, AURKA
GO:0007067	Mitotic nuclear division	3	0.002109580844250449	CDC20, CDK1, AURKA
GO:0045931	Positive regulation of mitotic cell cycle	2	0.00831053212854763	CCNB1, CDK1
CC				
GO:0005813	Centrosome	4	1.224777247874113E-4	CDC20, CCNB1, CDK1, AURKA
GO:0005654	Nucleoplasm	5	0.0023863917920581195	CDC20, CCNB1, CDK1, AURKA, ASF1B
GO:0005829	Cytosol	5	0.004671535818422827	CDC20, CCNB1, CDK1, HMMR, AURKA
GO:0072686	Mitotic spindle	2	0.011199624811404262	CDK1, AURKA
GO:0005876	Spindle microtubule	2	0.012015152655811594	CDK1, AURKA
MF				
GO:0035173	Histone kinase activity	2	0.0011843428611568918	CCNB1, CDK1
GO:0004693	Cyclin-dependent protein serine/threonine kinase activity	2	0.010031192883095138	CCNB1, CDK1
GO:0005515	Protein binding	6	0.03814879524822187	CDC20, CCNB1, CDK1, HMMR, AURKA, ASF1B

Table 4. Details of the KEGG pathway analysis of identified hub genes extracted from various GEO PRAD expression microarray datasets

Pathway ID	Pathway Name	Gene count	*P*-value	Gene name
hsa04114	Oocyte meiosis	4	1.616848175824832E-5	CDC20, CCNB1, CDK1, AURKA
hsa04110	Cell cycle	3	0.0018887038532489457	CDC20, CCNB1, CDK1
hsa04115	p53 signaling pathway	2	0.038401909244846745	CCNB1, CDK1
hsa04914	Progesterone-mediated oocyte maturation	2	0.0496477278983673	CCNB1, CDK1
hsa05203	Viral carcinogenesis	2	0.04970365119958482	CDC20, CDK1

TFS-miRNA-mRNA network

TFS-miRNA-real network of real hub genes was constructed in this study by ENCORI and displayed by Cytoscape. In the constructed network, we identified degree of centrality based one TF (E2F1), and one miRNA (hsa-mir-124-3p) as the most crucial TF and miRNA due to their ability to target all six real hub genes. Therefore, the explored TFS-miRNAs-real hub genes co-regulatory network in this study has shown that the E2F1-hsa-mir-124-3p/CDC20/HMR/AURKA/CDK1/ASF1B/CCNB1 axis is a possible inducer of PRAD. For further verification of the identified TF and miRNA roles in inducing PRAD by up-regulating the real hub genes, the expressions of E2F1 and has-mir-124-3p in PRAD samples relative to controls were checked by UALCAN and dbDEMC, respectively. Results of the analysis showed a significant up-regulation of E2F1 and down-regulation of hsa-mir-124-3p was also observed in PRAD samples relative to normal controls. In light of this evidence, we suggested that up-regulated E2F1 and down-regulated has-miR-124-3p may also exert PRAD inducing effects by up-regulating their target real hub genes (**Figure 10**).

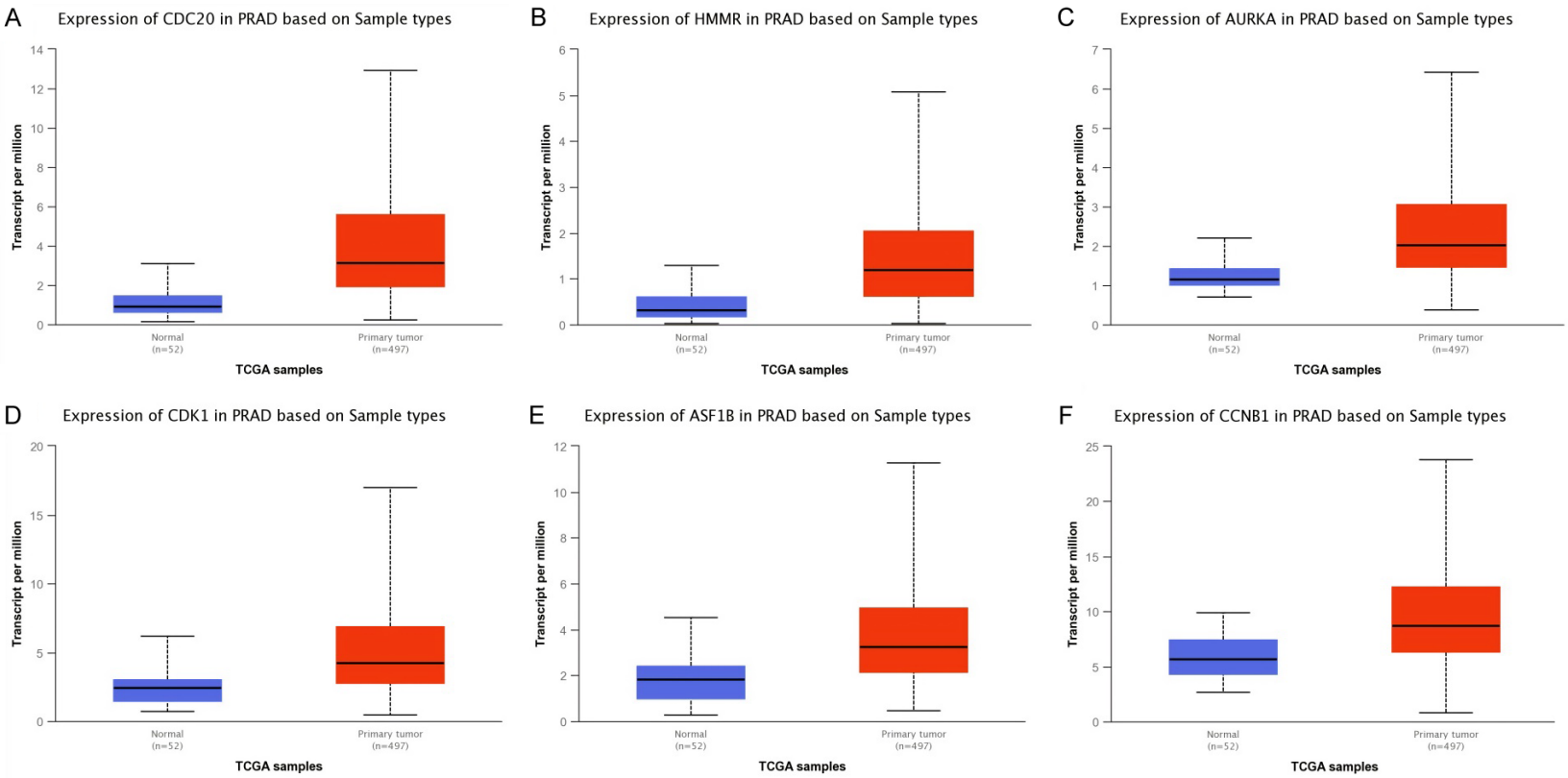

Figure 3. UALCAN-based transcription expression of real hub genes across PRAD and normal controls. (A) CDC20, (B) HMMR, (C) AURKA, (D) CDK1, (E) ASF1B, and (F) CCNB1. A *p*-value <0.05 was considered significant.

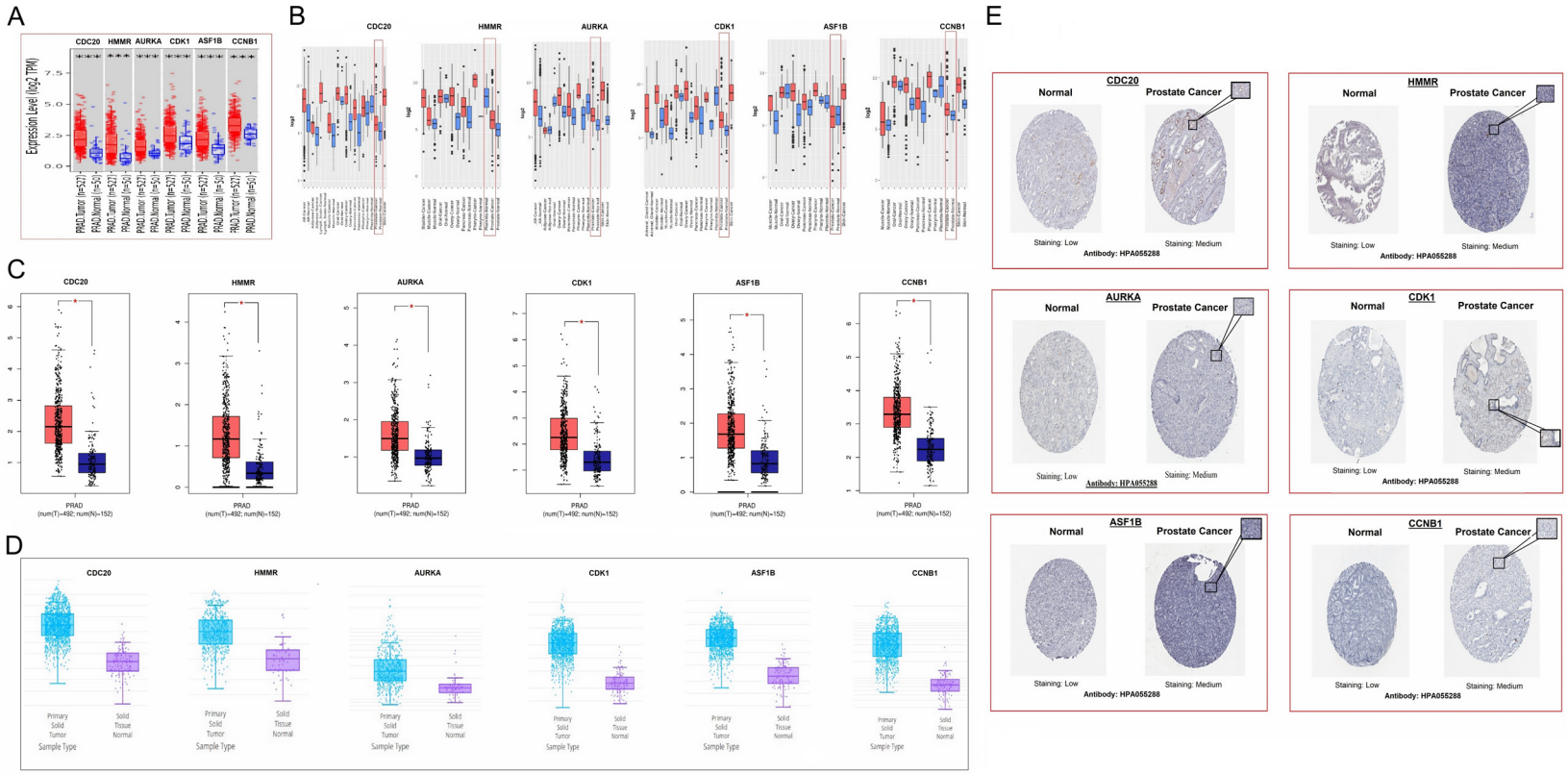

Figure 4. Transcription and protein expression validations of the real hub genes via different additional databases. (A) Via TIMER, (B) Via GENT2, (C) Via GEPIA, (D) Via DriverDBV3, and (E) Via HPA. In HPA, low level of real hub genes staining was observed in normal Prostate tissues, while medium higher level was seen in PRAD tissues. The magnification of HPA-based the images are ×200, and the scale bars are 100 μm. A *p*-value <0.05 was considered significant.

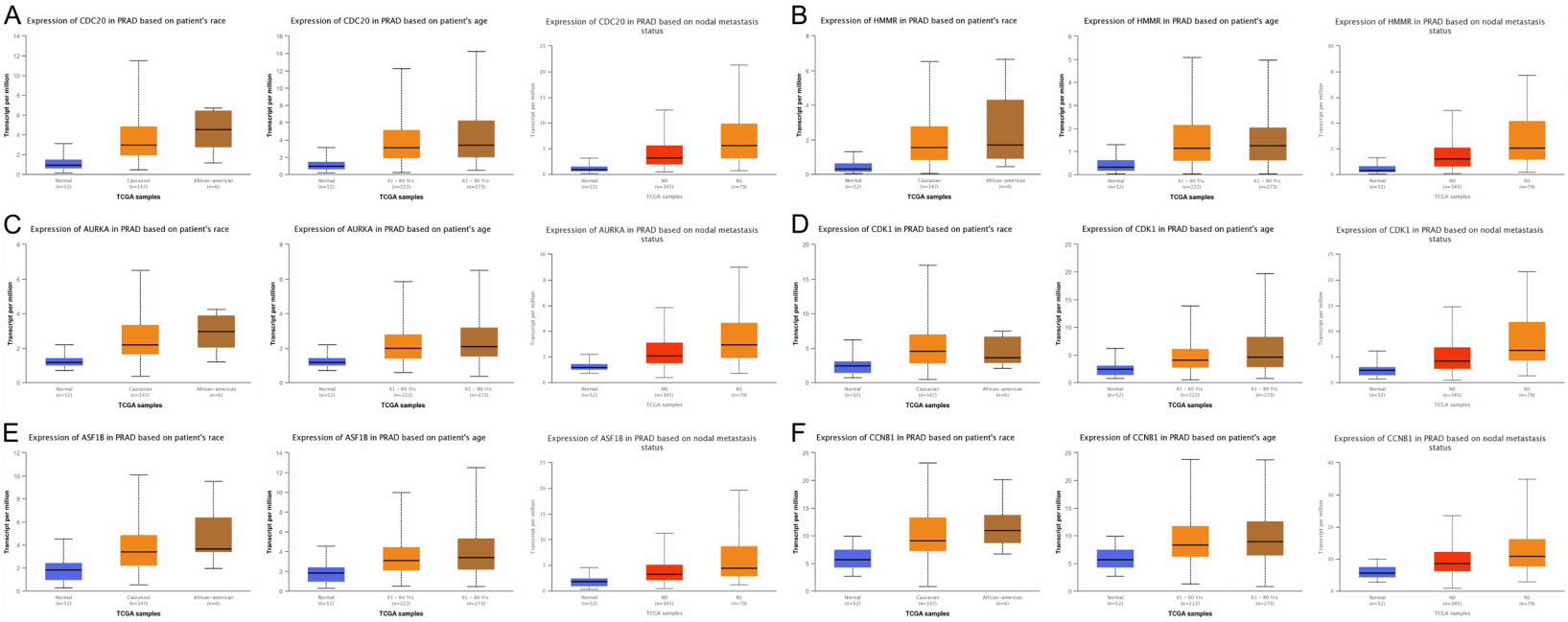

Figure 5. Transcription expression of real hub genes across PRAD patients stratified by different clinicopathological features. (A) Across PRAD patients of different race, age groups, and nodal metastasis, (B) Across PRAD patients of different race, age groups, and nodal metastasis, (C) Across PRAD patients of different race, age groups, and nodal metastasis, (D) Across PRAD patients of different race, age groups, and nodal metastasis, (E) Across PRAD patients of different race, age groups, and nodal metastasis, and (F) Across PRAD patients of different race, age groups, and nodal metastasis. A *p*-value <0.05 was considered significant.

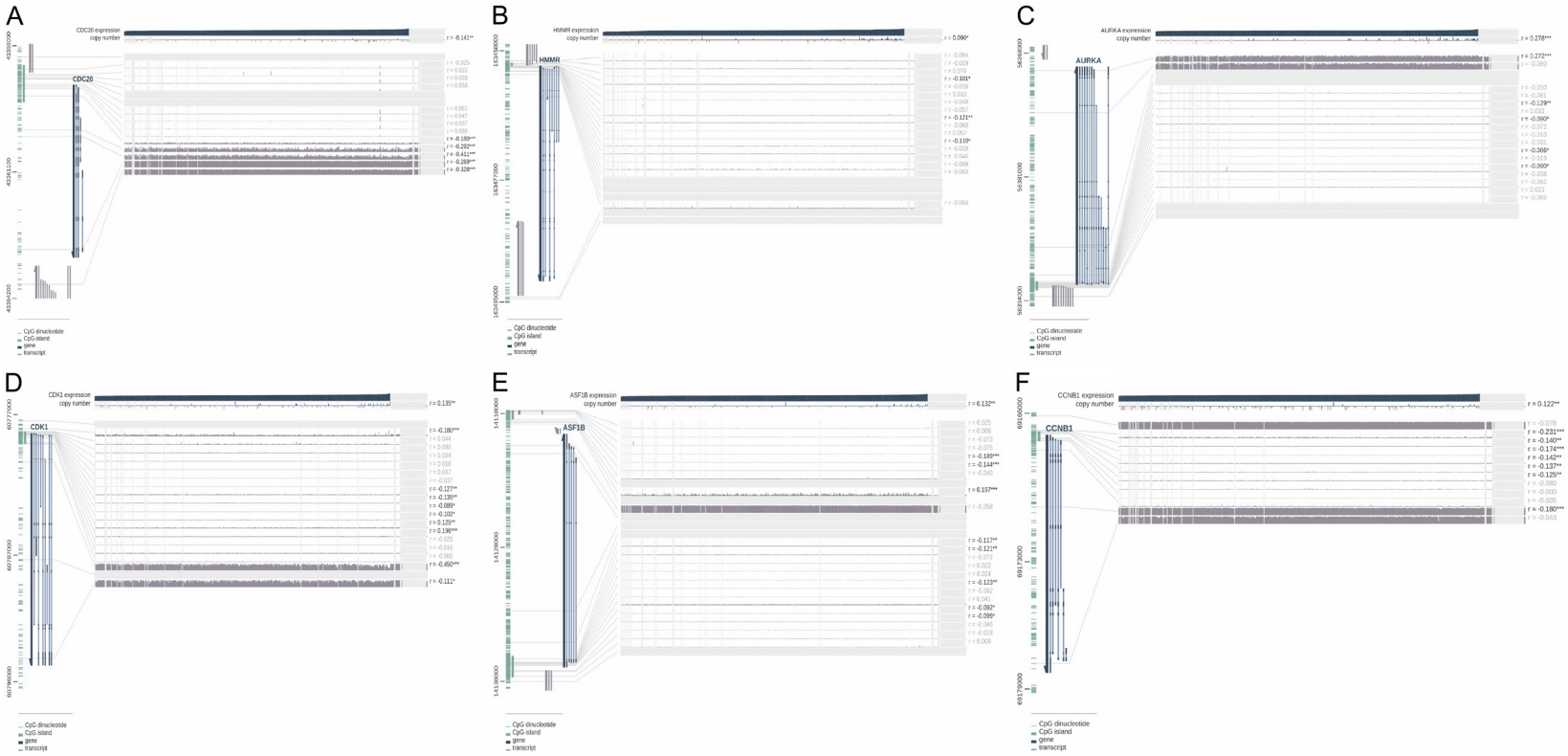

Figure 6. Correlation among the methylation levels of the promoter region and expression of real hub genes across PRAD samples paired with controls. (A) CDC20, (B) HMMR, (C) AURKA, (D) CDK1, (E) ASF1B, and (F) CCNB1. A *p*-value <0.05 was considered significant.

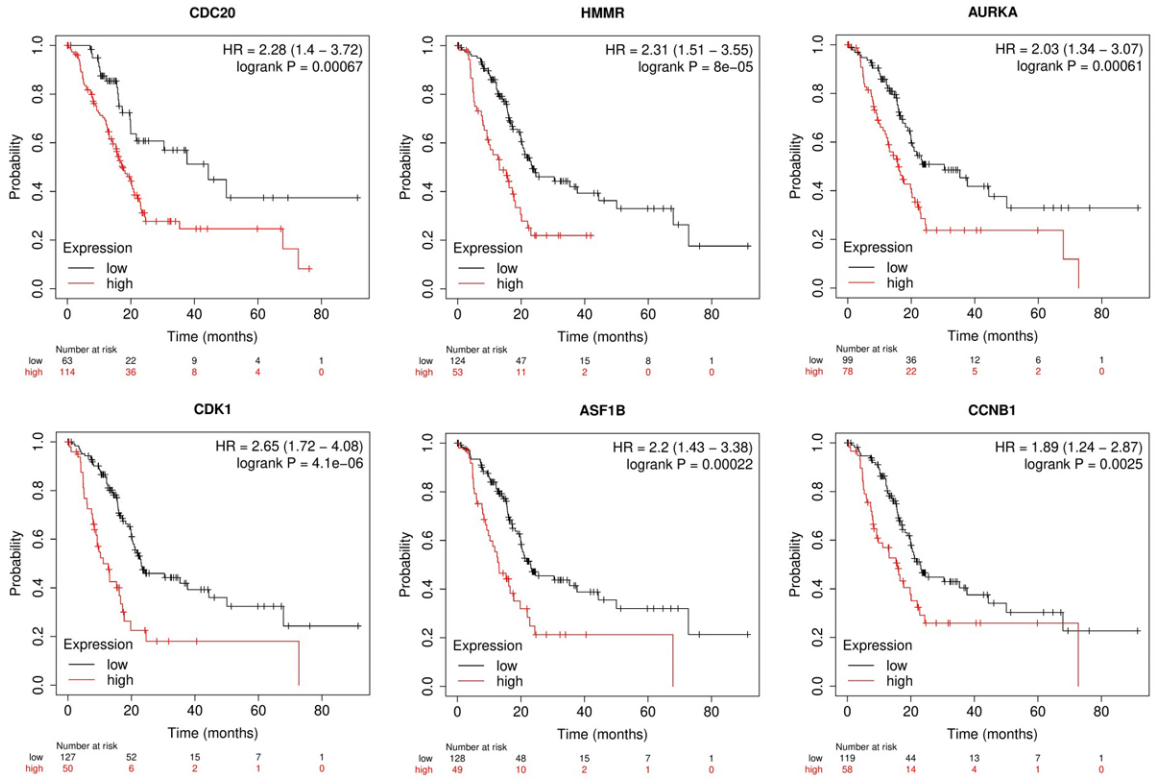

Figure 7. KM plotter-based OS analysis of real hub genes expression in PRAD patients. A *p*-value <0.05 was considered significant.

Single-cell functional analysis

CancerSEA has helped us in this study to further decode the important roles of real hub genes in PRAD at the single-cell level. In view of the analysis results, real hub genes (CDC20, HMMR, AURKA, CDK1, ASF1B, and CCNB1) were noted to be linked (positively or negatively) with fourteen different states (**Figure 11A**) in PRAD. However, out of these fourteen states, real hub genes expression was notably positively correlated with only Proliferation, DNA Damage, Invasion, Apoptosis, and Hypoxia (**Figure 11B**).

Real hub genes association with different other mutant genes

By MuTarget, top three mutant genes with FC>1.4, P<0.05, and somatic mutation rate >1% conditions were explored in this study. These positively correlated mutant genes with real hub genes expression are TP53, MYO9A, and KIF13A with CDC20, TP53, JAK1, and XIR2P with HMMR, TP53, XIR2P, and MYO9A with AURKA, TP53, JAK1, and XIR2P with CDK1, MYO3A, MYO9A, and JAK1 with ASF1B, and MUC17, JAK1, and XIR2P with CCNB1 (Supplementary Figure 1).

Novel drug prediction for real hub genes

Given the associations between real hub gene expression and PRAD outcome, we speculated that drugs potentially affecting real hub genes expression might be valuable in the antitumor treatment of PRAD. Therefore, we also searched for drugs targeting CDC20, HMMR, AURKA, CDK1, ASF1B, and CCNB1 to regulate their expression. For instance, estradiol and diethylnitrosamine were found in this study that can elevate CDC20 expression while aflatoxin B1 and bisphenol A are capable of reducing CDC20 expression level (Supplementary Figure 2).

Discussion

Prostatic adenocarcinoma (PRAD) is a tumor with complex characteristics and can be life-threatening if not diagnosed in time [34]. In this study, we explored a few more closely linked real hub genes with PRAD by utilizing already

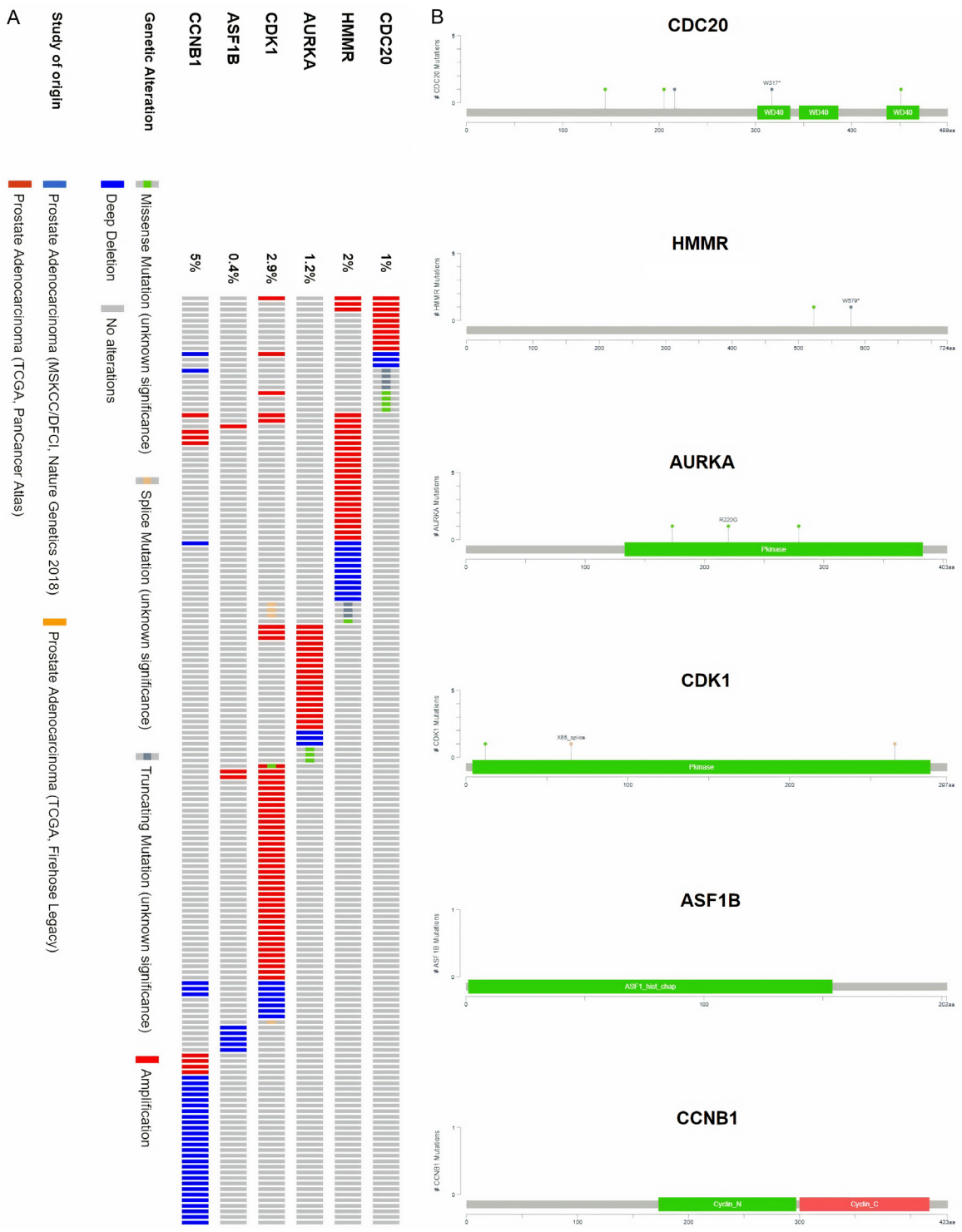

Figure 8. Frequency and distribution of genomic alterations associated with real hub genes in PRAD. (A) Frequency of genomic alteration, and (B) Distribution of mutations in protein domains of real hub genes.

reported hub genes based on PRAD GEO expression datasets. Initially, from 17 selected studies, we manually isolated 124 hub genes and combined them to get a consolidated pool. Next, a STRING-based PPI network of 124 hub genes was analyzed by Cytoscape to explore six significantly PRAD-related real hub genes by degree method. The top six selected real

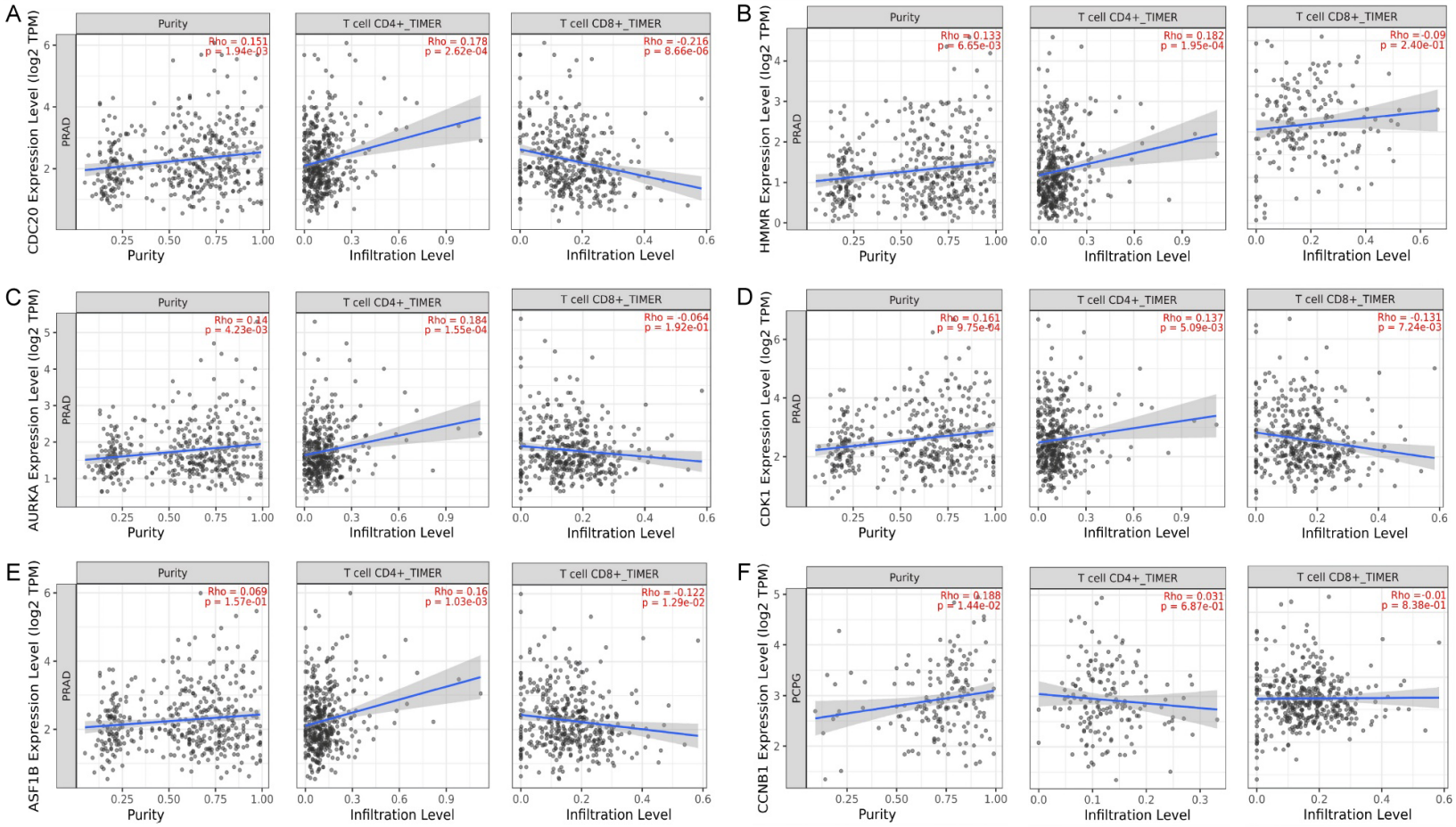

Figure 9. Correlation analysis of real hub genes expression with tumor purity, CD4+ T, and CD8+ T cells in PRAD. (A) CDC20, (B) HMMR, (C) AURKA, (D) CDK1, (E) ASF1B, and (F) CCNB1. A *p*-value <0.05 was considered significant.

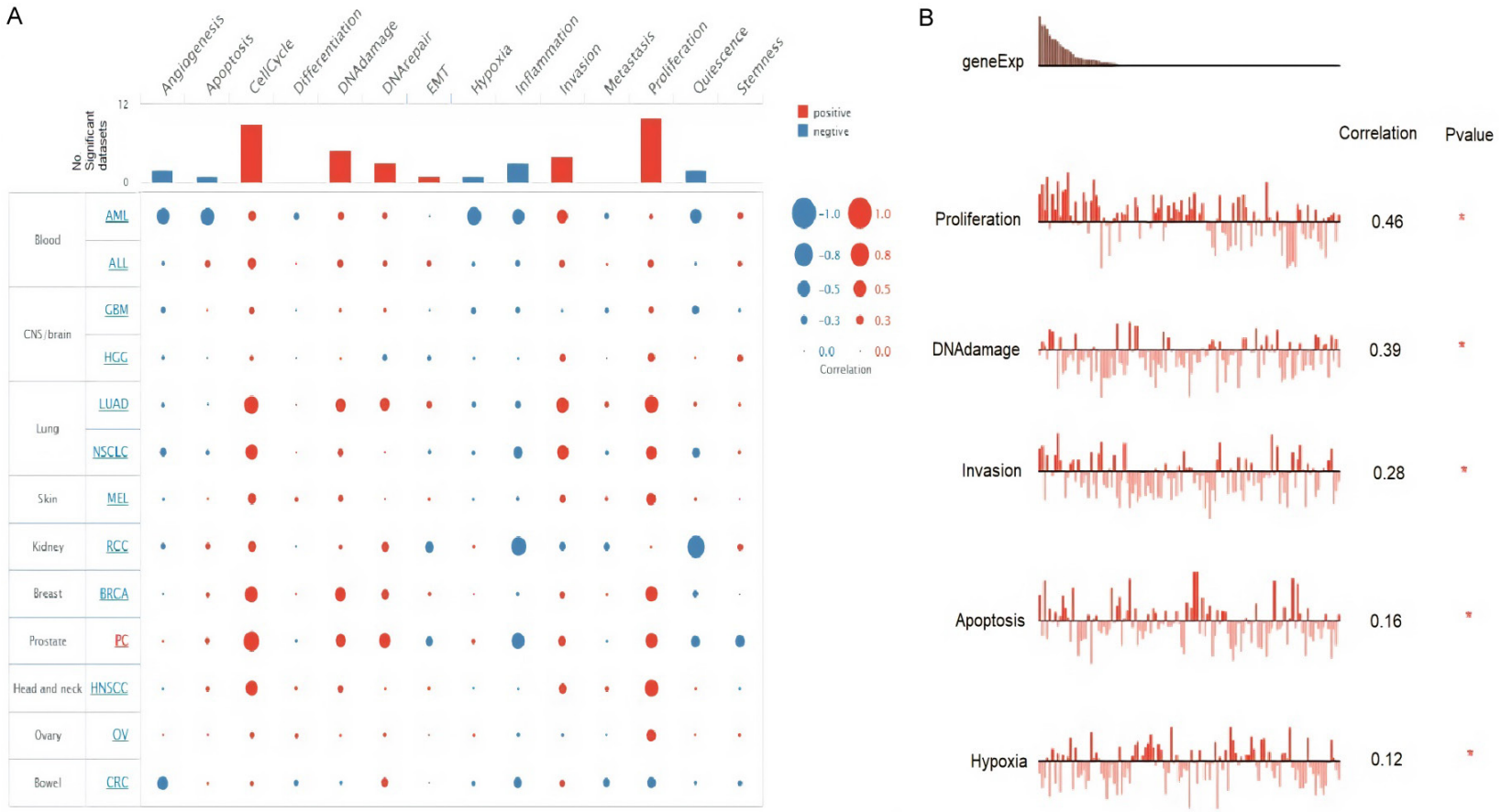

Figure 10. CancerSEA based correlations between real hub genes and different other states. (A) Correlation analysis of real hub genes expression with 14 different states in PRAD, and (B) Correlation analysis of real hub gene expression with only significant states in PRAD. A *p*-value <0.05 was considered significant.

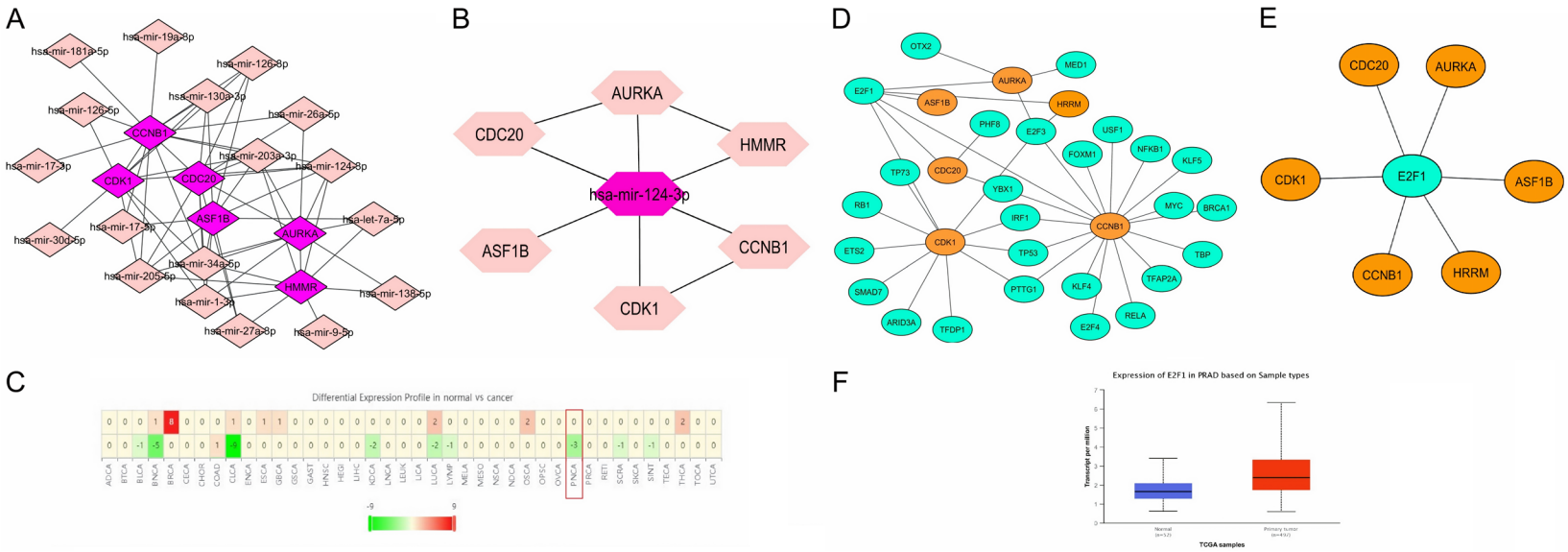

Figure 11. TF-miRNA-mRNA network analysis of real hub genes in PRAD. (A) miRNAs targeting real hub genes, (B) has-mir-124-3p miRNA targeting real hub genes, (C) Relative expression of has-mir-124-3p in PRAD and normal controls, (D) TFS targeting real hub genes, (E) EAF2 targeting real hub genes, and (F) Relative expression analysis of E2F1 in PRAD samples paired with controls. A *p*-value <0.05 was considered significant. The pink and orange nodes represent the real hub gene, purple nodes represent the miRNAs, while beryl nodes represent the TFS.

hub genes are CDC20, HMMR, AURKA, CDK1, ASF1B, and CCNB1. The GO and KEGG analysis of real hub genes revealed their significant (P<0.05) roles in diverse GO and KEGG terms (**Figure 2**).

CDC20 gene encodes for a CDC20 protein that exhibits ubiquitin ligase activity and acts as a critical factor for inhibiting S-M phase CDKs [35]. It is also a part of spindle assembly checkpoint protein to ensure activation of anaphase [36]. CDC20 acts as a proto-oncogene in promoting human carcinogenesis and its overexpression has been associated with the aggressiveness of prostate cancer [37], breast cancer [38], lung carcinogenesis [39], glioblastoma [40], head and neck cancer [41], urothelial bladder cancer [36], cervical squamous cell carcinoma [42], PDAC [43] gastric cancer [44, 45], tumor progression in hepatocellular carcinoma [46], and melanoma [47]. In the present study, we have observed the significant (P< 0.05) overexpression of CDC20 across PRAD samples of different clinicopathologic characteristics relative to controls.

HMMR, also called CD168, encodes a protein that is involved in cell motility and acts as a receptor for hyaluronic acid (HA) [48]. Upon binding with HA, HMMR interacts with microtubules, regulates mitosis, and results in cellular transformation by activating ERK1/2-MEK1 and MAPK pathways [49]. HMMR is over-expressed in many cancers and results in the development and progression of tumors. Earlier, the up-regulation of HMMR was reported in prostate cancer [50], acute lymphoid leukemia and acute myeloid leukemia (AML) [51], epithelial ovarian cancer [52], esophageal adenocarcinoma [53], and head and neck carcinoma [54]. In our study, we found its significant (P<0.05) up-regulation across PRAD patients with different clinical characteristics relative to controls.

AURKA is a serine/threonine kinase that helps in cell cycle regulation [55]. AURKA overexpression has been associated with different cancers including prostate cancer [56], breast cancer [57] colon tumorigenesis [58], gastric cancer [59], head and neck cancer [60], liver metastasis [61], hepatocarcinogenesis [62], bladder cancer [63], NSCLC progression [64], ovarian cells [65], and esophageal cancer [66]. Moreover, many subsequent studies have also been carried out to evaluate the AURKA expression level in PRAD, still, its role is poorly understood. In the current study, we have documented the significant (P<0.05) up-regulation of AURKA in PRAD patients with different clinical characteristics relative to controls.

CDC2 gene encodes for CDK1, which is a cell cycle checkpoint and also helps in cell cycle regulation [67]. Up-regulated CDK1 is known as an inducer of prostate cancer [68], breast cancer [69, 70], lung cancer [71, 72], thyroid cancer [73], cervical cancer [74], oral squamous cell carcinoma [75], melanomas [76], pancreatic ductal adenocarcinoma (PDAC) [77], ovarian cancer [78, 79], and hepatocellular carcinoma [80]. In our study, we found that CDK1 was significantly (P<0.05) overexpressed in PRAD patients with different clinical characteristics relative to controls.

ASF1B encodes for a member of the H3/H4 histone family [81], which is involved in mediating nucleosome structure by constant histone supply and replication-dependent chromatin assembly [82]. ASF1B up-regulation has already been reported in many cancers, such as prostate cancer [83] breast cancer [84], gastrointestinal cancer [85], renal cancer [86, 87], lung cancer [88], cervical cancer [89], colorectal cancer [90], bladder cancer, head and neck cancer, brain, and central nervous system cancers [91]. In contrast, a study has also reported that the higher expression of ASF1B in gastric cancer inhibits its proliferation by the Bax/Bcl-2-p53 pathway [92]. In the current study, we have documented the significant (P<0.05) up-regulation of ASF1B in PRAD patients with different clinicopathologic features relative to controls.

CCNB1 encodes for the mitotic regulatory protein cyclin B1, which forms a maturation-promoting factor with CDC2 to control the G2-M transition phase of the cell cycle [93]. CCNB1 up-regulation has been found to be associated with various cancers including prostate cancer [94], colorectal cancer [95], oral carcinoma [96], hepatocellular carcinoma [97], gastric cancer [98], esophageal cancer [99], NSCLC [100, 101], pancreatic cancer [102], cervical cancer [103], and rhabdomyosarcoma [104]. In this study, we found its significant (P<0.05) up-regulation in PRAD patients of different clinical characteristics as compared to the normal con-

trols. Taken together, using expression profiling of the real hub genes including CDC20, HMMR, AURKA, CDK1, ASF1B, and CCNB1, we have suggested that up-regulation of these six genes may serve as a potential biomarker in PRAD patients regardless of different clinical characteristics relative to controls. The results of correlational analysis between the mRNA expression of the real hub genes OS duration of the PRAD patients showed that overexpression of the real hub genes served as a good prognostic factor for measuring the OS of PRAD patients, suggesting the application of these genes as prognostic biomarkers.

Through genetic alteration analysis, our research revealed that real hub genes genetically altered or gain and lose their copies in the very low proportion of the PRAD patients. In addition, it was also observed that mutations in the real hub genes (CDC20, HMMR, AURKA, and CDK1) can alter amino acids at different positions in the resultant proteins. Furthermore, the correlational analysis between the mRNA expression and promoter methylation level of the real hub genes in PRAD revealed the expected significant ($P<0.05$) negative correlation. Therefore, it is speculated that promoter hypomethylation might have played a significant role in the up-regulation of real hub genes in PRAD.

The key components of anticancer immunity are tumor purity, CD4+ T, and CD8+ T immune cells [105]. In the current research, we found correlations among tumor purity, CD4+ T immune cell infiltration, CD8+ T immune cell infiltration, and real hub gene expression in PRAD. Results have shown that real hub genes have a positive correlation with tumor purity and CD4+ T immune cell infiltration in PRAD, while a negative correlation with CD8+ T immune cells infiltration. Previously, CD4+ T and CD8+ T immune cells infiltrations were used as a marker in laryngeal squamous cell carcinoma [106]. Moreover, CD8+ T and CD4+ T immune cell infiltration were also utilized successfully for the personalized immunotherapy treatment of LSCC [107]. Importantly, prior to our knowledge, this research is the first to explore the correlations between real hub gene expression (CDC20, HMMR, AURKA, CDK1, ASF1B, CCNB1) and CD4+ T and CD8+ T immune cells infiltration in PRAD. These correlations may bring new ideas for the personalized treatment of PRAD.

Through TFS-miRNA-real hub genes co-regulatory analysis, we observed that one TF (E2F1) and one miRNA (has-miR-124-3p) target all six real hub genes. It is already acknowledged by the previous studies that 5 miRNAs including has-miR-23b has-miR-20a, has-let-7d has-miR-20b, and has-let-7a, 6 mRNAs including VEGFA, TGFBR1, PIK3R1, EGFR, DLG4, and KIT, and 2 TFS including NR3C1, NRG1 are the important modulators of the PRAD [108]. In view of the results of the present study, we suggest that E2F1-has-miR-124-3p/CDC20/HMMR/AURKA/CDK1/ASF1B/CCNB1 TFS-miRNAs-real hub genes co-regulatory networks can also be used as new molecular biomarkers in PRAD. Moreover, the identified axis can also be used as therapeutic targets in the treatment of PRAD for regulating the gene expression of the real hub genes. As far as we know, this research is the first to report tumorigenesis roles of E2F1, and has-miR-124-3p together with CDC20, HMMR, AURKA, CDK1, ASF1B, CCNB1 in PRAD.

To understand the in-depth biological roles of real hub genes in PRAD development, we utilized the cancerSEA database to analyze their correlation with 14 different states in PRAD at the single-cell level. In view to our results, real hub genes were significantly positively correlated with Proliferation, DNA Damage, Invasion, Apoptosis, and Hypoxia in PRAD. To the best of our knowledge, this research is the first to collectively investigate the roles of identified hub genes in PRAD development with respect to Proliferation, DNA Damage, Invasion, Apoptosis, and Hypoxia.

Usually, prostate cancer patients harboring a variety of somatic mutations yet do not have appropriate targeted therapies [126]. Therefore, in our study, we expanded the real hub genes network using the muTarget platform to identify mutant genes that alter the expression of real hub genes. The top 3 mutant genes which positively correlated with the expression of each real hub gene are TP53, MYO9A, and KIF13A with CDC20, TP53, JAK1, and XIR2P with HMMR, TP53, XIR2P, and MYO9A with AURKA, TP53, JAK1, and XIR2P with CDK1, MYO3A, MYO9A, and JAK1 with ASF1B, and MUC17, JAK1, and XIR2P with CCNB1. This type of link between mutant genes and real hub genes expression may be helpful in designing multi-gene and personalized therapeutic strategies for PRAD patients. In addition, we have

identified a few drugs that could target the real hub genes and may affect the abnormal expression level, and could be part of therapeutic strategies.

Conclusion

Heterogeneity-specific barriers offered by cancer cells is one of the main issue limiting the effective diagnosis, predication of prognosis, and the efficiency of treatment outcomes. Collectively, our results have led us to the identification of six real hub genes which can be used for lowering heterogenetic-specific barriers in PRAD patients for accurate diagnosis and predicting the prognosis more precisely. Furthermore, the findings of this study may also enhance our understanding of PRAD development and progression and help to identify therapeutic targets for the better treatment.

Acknowledgements

The authors extend their appreciation to the Researchers Supporting Project number (RSP2022R470), King Saud University, Riyadh, Saudi Arabia.

Disclosure of conflict of interest

None.

Address correspondence to: Hamid Yaz and Mostafa A Abdel-Maksoud, Department of Botany and Microbiology, College of Science, King Saud University, Riyadh, P.O. 2455, Riyadh 11451, Saudi Arabia. E-mail: HYazSA@outlook.com (HY); harrany@gmail.com (MAAM)

References

[1] Siegel RL, Miller KD, Fuchs HE and Jemal A. Cancer statistics, 2021. CA Cancer J Clin 2021; 71: 7-33.

[2] Mei W, Lin X, Kapoor A, Gu Y, Zhao K and Tang D. The contributions of prostate cancer stem cells in prostate cancer initiation and metastasis. Cancers 2019; 11: 434.

[3] Fujita K, Hayashi T, Matsushita M, Uemura M and Nonomura N. Obesity, inflammation, and prostate cancer. J Clin Med 2019; 8: 201.

[4] Shiao SL, Chu GC and Chung LW. Regulation of prostate cancer progression by the tumor microenvironment. Cancer Lett 2016; 380: 340-348.

[5] Polotti CF, Kim CJ, Chuchvara N, Polotti AB, Singer EA and Elsamra S. Androgen deprivation therapy for the treatment of prostate cancer: a focus on pharmacokinetics. Expert Opin Drug Metab Toxicol 2017; 13: 1265-1273.

[6] Barani M, Sabir F, Rahdar A, Arshad R and Kyzas GZ. Nanotreatment and nanodiagnosis of prostate cancer: recent updates. Nanomaterials 2020; 10: 1696.

[7] Hudson MA, Bahnson RR and Catalona WJ. Clinical use of prostate specific antigen in patients with prostate cancer. J Urol 1989; 142: 1011-1017.

[8] Phé V, Cussenot O and Rouprêt M. Methylated genes as potential biomarkers in prostate cancer. BJU Int 2010; 105: 1364-1370.

[9] Loeb S, Bjurlin MA, Nicholson J, Tammela TL, Penson DF, Carter HB, Carroll P and Etzioni R. Overdiagnosis and overtreatment of prostate cancer. Eur Urol 2014; 65: 1046-1055.

[10] Prokhnevska N, Emerson DA, Kissick HT and Redmond WL. Immunological complexity of the prostate cancer microenvironment influences the response to immunotherapy. Adv Exp Med Biol 2019; 1210: 121-147.

[11] Ceci F, Fiorentino M, Castellucci P and Fanti S. Molecular imaging and precision medicine in prostate cancer. PET Clin 2017; 12: 83-92.

[12] Olivier C and Bernard M. Biomarkers of aggressiveness in prostate cancer. Prostate cancer-diagnostic and therapeutic advances. Rijeka, Croatia: InTech; 2011. pp.3-20.

[13] Leslie S, Soon-Sutton T, Sajjad H and Siref L. Prostate Cancer. In: StatPearls. Treasure Island (FL): StatPearls; 2022.

[14] Feng T, Wei D, Li Q, Yang X, Han Y, Luo Y and Jiang Y. Four novel prognostic genes related to prostate cancer identified using co-expression structure network analysis. Front Genet 2021; 12: 584164.

[15] Clough E and Barrett T. The gene expression omnibus database. Methods Mol Biol 2016; 1418: 93-110.

[16] Zhao X, Hu D, Li J, Zhao G, Tang W and Cheng H. Database mining of genes of prognostic value for the prostate adenocarcinoma microenvironment using the cancer gene atlas. Biomed Res Int 2020; 2020: 5019793-5019793.

[17] Zhao X, Lei Y, Li G, Cheng Y, Yang H, Xie L, Long H and Jiang R. Integrative analysis of cancer driver genes in prostate adenocarcinoma. Mol Med Rep 2019; 19: 2707-2715.

[18] Szklarczyk D, Gable AL, Lyon D, Junge A, Wyder S, Huerta-Cepas J, Simonovic M, Doncheva NT, Morris JH, Bork P, Jensen LJ and Mering CV. STRING v11: protein-protein association networks with increased coverage, supporting functional discovery in genome-wide experimental datasets. Nucleic Acids Res 2019; 47: D607-D613.

[19] Shannon P, Markiel A, Ozier O, Baliga NS, Wang JT, Ramage D, Amin N, Schwikowski B and Ideker T. Cytoscape: a software environment for integrated models of biomolecular interaction networks. Genome Res 2003; 13: 2498-2504.
[20] Chandrashekar DS, Bashel B, Balasubramanya SAH, Creighton CJ, Ponce-Rodriguez I, Chakravarthi B and Varambally S. UALCAN: a portal for facilitating tumor subgroup gene expression and survival analyses. Neoplasia 2017; 19: 649-658.
[21] Jézéquel P, Campone M, Gouraud W, Guérin-Charbonnel C, Leux C, Ricolleau G and Campion L. bc-GenExMiner: an easy-to-use online platform for gene prognostic analyses in breast cancer. Breast Cancer Res Treat 2012; 131: 765-775.
[22] Park SJ, Yoon BH, Kim SK and Kim SY. GENT2: an updated gene expression database for normal and tumor tissues. BMC Med Genomics 2019; 12: 101.
[23] Chung IF, Chen CY, Su SC, Li CY, Wu KJ, Wang HW and Cheng WC. DriverDBv2: a database for human cancer driver gene research. Nucleic Acids Res 2016; 44: D975-D979.
[24] Thul PJ and Lindskog C. The human protein atlas: a spatial map of the human proteome. Protein Sci 2018; 27: 233-244.
[25] Koch A, De Meyer T, Jeschke J and Van Criekinge W. MEXPRESS: visualizing expression, DNA methylation and clinical TCGA data. BMC Genomics 2015; 16: 636.
[26] Szász AM, Lánczky A, Nagy Á, Förster S, Hark K, Green JE, Boussioutas A, Busuttil R, Szabó A and Győrffy B. Cross-validation of survival associated biomarkers in gastric cancer using transcriptomic data of 1,065 patients. Oncotarget 2016; 7: 49322.
[27] Cerami E, Gao J, Dogrusoz U, Gross BE, Sumer SO, Aksoy BA, Jacobsen A, Byrne CJ, Heuer ML, Larsson E, Antipin Y, Reva B, Goldberg AP, Sander C and Schultz N. The cBio cancer genomics portal: an open platform for exploring multidimensional cancer genomics data. Cancer Dis 2012; 2: 401-404.
[28] Li T, Fu J, Zeng Z, Cohen D, Li J, Chen Q, Li B and Liu XS. TIMER2.0 for analysis of tumor-infiltrating immune cells. Nucleic Acids Res 2020; 48: W509-W514.
[29] Huang DP, Zeng YH, Yuan WQ, Huang XF, Chen SQ, Wang MY, Qiu YJ and Tong GD. Bioinformatics analyses of potential miRNA-mRNA regulatory axis in HBV-related hepatocellular carcinoma. Int J Med Sci 2021; 18: 335-346.
[30] Yang Z, Wu L, Wang A, Tang W, Zhao Y, Zhao H and Teschendorff AE. dbDEMC 2.0: updated database of differentially expressed miRNAs in human cancers. Nucleic Acids Res 2017; 45: D812-D818.
[31] Yuan H, Yan M, Zhang G, Liu W, Deng C, Liao G, Xu L, Luo T, Yan H, Long Z, Shi A, Zhao T, Xiao Y and Li X. CancerSEA: a cancer single-cell state atlas. Nucleic Acids Res 2019; 47: D900-D908.
[32] Nagy Á and Győrffy B. muTarget: a platform linking gene expression changes and mutation status in solid tumors. Int J Cancer 2021; 148: 502-511.
[33] Mattingly CJ, Colby GT, Forrest JN and Boyer JL. The comparative toxicogenomics database (CTD). Environ Health Perspect 2003; 111: 793-795.
[34] Autier P. Risk factors and biomarkers of life-threatening cancers. Ecancermedicalscience 2015; 9: 596-596.
[35] Kramer ER, Gieffers C, Hölzl G, Hengstschläger M and Peters JM. Activation of the human anaphase-promoting complex by proteins of the CDC20/Fizzy family. Curr Biol 1998; 8: 1207-10.
[36] Choi JW, Kim Y, Lee JH and Kim YS. High expression of spindle assembly checkpoint proteins CDC20 and MAD2 is associated with poor prognosis in urothelial bladder cancer. Virchows Arch 2013; 463: 681-687.
[37] Zhang Q, Huang H, Liu A, Li J, Liu C, Sun B, Chen L, Gao Y, Xu D and Su C. Cell division cycle 20 (CDC20) drives prostate cancer progression via stabilization of β-catenin in cancer stem-like cells. EBioMedicine 2019; 42: 397-407.
[38] Karra H, Repo H, Ahonen I, Löyttyniemi E, Pitkänen R, Lintunen M, Kuopio T, Söderström M and Kronqvist P. Cdc20 and securin overexpression predict short-term breast cancer survival. Br J Cancer 2014; 110: 2905-2913.
[39] Zhang MY, Liu XX, Li H, Li R, Liu X and Qu YQ. Elevated mRNA levels of AURKA, CDC20 and TPX2 are associated with poor prognosis of smoking related lung adenocarcinoma using bioinformatics analysis. Int J Med Sci 2018; 5: 1676-1685.
[40] Ji P, Smith S, Wang Y, Jiang R, Song S, Li B, Sawaya R, Bruner J, Kuang J, Yu H, Fuller GN and Zhang W. Inhibition of gliomagenesis and attenuation of mitotic transition by MIIP. Oncogene 2010; 29: 3501-3508.
[41] Mondal G, Sengupta S, Panda CK, Gollin SM, Saunders WS and Roychoudhury S. Overexpression of Cdc20 leads to impairment of the spindle assembly checkpoint and aneuploidization in oral cancer. Carcinogenesis 2007; 28: 81-92.
[42] Kim Y, Choi JW, Lee JH and Kim YS. MAD2 and CDC20 are upregulated in high-grade squamous intraepithelial lesions and squamous cell carcinomas of the uterine cervix. Int J Gynecol Pathol 2014; 33: 517-523.

[43] Dong S, Huang F, Zhang H and Chen Q. Overexpression of BUB1B, CCNA2, CDC20, and CDK1 in tumor tissues predicts poor survival in pancreatic ductal adenocarcinoma. Biosci Rep 2019; 39: BSR20182306.
[44] Chang DZ, Ma Y, Ji B, Liu Y, Hwu P, Abbruzzese JL, Logsdon C and Wang H. Increased CDC20 expression is associated with pancreatic ductal adenocarcinoma differentiation and progression. J Hematol Oncol 2012; 5: 1-7.
[45] Ding ZY, Wu HR, Zhang JM, Huang GR and Ji DD. Expression characteristics of CDC20 in gastric cancer and its correlation with poor prognosis. Int J Clin Exp Pathol 2014; 7: 722.
[46] Li J, Gao JZ, Du JL, Huang ZX and Wei LX. Increased CDC20 expression is associated with development and progression of hepatocellular carcinoma. Int J Oncol 2014; 45: 1547-1555.
[47] Majumder P, Bhunia S, Bhattacharyya J and Chaudhuri AJ. Inhibiting tumor growth by targeting liposomally encapsulated CDC20siRNA to tumor vasculature: therapeutic RNA interference. J Control Release 2014; 180: 100-108.
[48] Hardwick C, Hoare K, Owens R, Hohn H, Hook M, Moore D, Cripps V, Austen L, Nance D and Turley E. Molecular cloning of a novel hyaluronan receptor that mediates tumor cell motility. J Cell Biol 1992; 117: 1343-1350.
[49] Tolg C, Hamilton SR, Morningstar L, Zhang J, Zhang S, Esguerra KV, Telmer PG, Luyt LG, Harrison R, McCarthy JB and Turley EA. RHAMM promotes interphase microtubule instability and mitotic spindle integrity through MEK1/ERK1/2 activity. J Biol Chem 2010; 285: 26461-26474.
[50] Rizzardi AE, Vogel RI, Koopmeiners JS, Forster CL, Marston LO, Rosener NK, Akentieva N, Price MA, Metzger GJ, Warlick CA, Henriksen JC, Turley EA, McCarthy JB and Schmechel SC. Elevated hyaluronan and hyaluronan-mediated motility receptor are associated with biochemical failure in patients with intermediate-grade prostate tumors. Cancer 2014; 120: 1800-1809.
[51] Spranger S, Jeremias I, Wilde S, Leisegang M, Stärck L, Mosetter B, Uckert W, Heemskerk MH, Schendel DJ and Frankenberger B. TCR-transgenic lymphocytes specific for HMMR/Rhamm limit tumor outgrowth in vivo. Am J Hematol 2012; 119: 3440-3449.
[52] Chu Z, Dai J, Jia L, Li J, Zhang Y, Zhang Z and Yan P. Increased expression of long noncoding RNA HMMR-AS1 in epithelial ovarian cancer: an independent prognostic factor. Eur Rev Med Pharmacol Sci 2018; 22: 8145-8150.
[53] Kang H, Wang N, Wang X, Zhang Y, Lin S, Mao G, Liu D, Dang C and Zhou Z. A glycolysis-related gene signature predicts prognosis of patients with esophageal adenocarcinoma. Aging 2020; 12: 25828.
[54] Lu T, Zheng Y, Gong X, Lv Q, Chen J, Tu Z, Lin S, Pan J, Guo Q and Li J. High expression of hyaluronan-mediated motility receptor predicts adverse outcomes: a potential therapeutic target for head and neck squamous cell carcinoma. Front Oncol 2021; 11: 499.
[55] Crane R, Gadea B, Littlepage L, Wu H and Ruderman JV. Aurora A, meiosis and mitosis. Biol Cell 2004; 96: 215-229.
[56] Nouri M, Ratther E, Stylianou N, Nelson CC, Hollier BG and Williams ED. Androgen-targeted therapy-induced epithelial mesenchymal plasticity and neuroendocrine transdifferentiation in prostate cancer: an opportunity for intervention. Front Oncol 2014; 4: 370.
[57] Dai ZJ, Kang HF, Wang XJ, Shao YP, Lin S, Zhao Y, Ren HT, Min WL, Wang M and Liu XX. Association between genetic polymorphisms in AURKA (rs2273535 and rs1047972) and breast cancer risk: a meta-analysis involving 37,221 subjects. Cancer Cell Int 2014; 14: 1-8.
[58] Takahashi Y, Sheridan P, Niida A, Sawada G, Uchi R, Mizuno H, Kurashige J, Sugimachi K, Sasaki S, Shimada Y, Hase K, Kusunoki M, Kudo S, Watanabe M, Yamada K, Sugihara K, Yamamoto H, Suzuki A, Doki Y, Miyano S, Mori M and Mimori K. The AURKA/TPX2 axis drives colon tumorigenesis cooperatively with MYC. Ann Oncol 2015; 26: 935-942.
[59] Sehdev V, Katsha A, Arras J, Peng D, Soutto M, Ecsedy J, Zaika A, Belkhiri A and El-Rifai W. HDM2 regulation by AURKA promotes cell survival in gastric cancer. Clin Cancer Res 2014; 20: 76-86.
[60] Chou CH, Yang NK, Liu TY, Tai SK, Hsu DS, Chen YW, Chen YJ, Chang CC, Tzeng CH and Yang MH. Chromosome instability modulated by BMI1-AURKA signaling drives progression in head and neck cancer. Cancer Res 2013; 73: 953-966.
[61] Goos JA, Coupé VM, Diosdado B, Delis-van Diemen PM, Karga C, Beliën JA, Carvalho B, van den Tol MP, Verheul HM and Geldof AA. Aurora kinase A (AURKA) expression in colorectal cancer liver metastasis is associated with poor prognosis. Br J Cancer 2013; 109: 2445-2452.
[62] Su ZL, Su CW, Huang YL, Yang WY, Sampurna BP, Ouchi T, Lee KL, Wu CS, Wang HD and Yuh CH. A novel AURKA mutant-induced early-onset severe hepatocarcinogenesis greater than wild-type via activating different pathways in zebrafish. Cancers 2019; 11: 927.
[63] Long Q, An X, Chen M, Wang N, Sui S, Li Y, Zhang C, Lee K, Wang X and Tian T. PUF60/AURKA axis contributes to tumor progression and malignant phenotypes in bladder cancer. Front Oncol 2020; 10: 2056.

[64] Schneider MA, Christopoulos P, Muley T, Warth A, Klingmueller U, Thomas M, Herth FJ, Dienemann H, Mueller NS and Theis F. AURKA, DLGAP5, TPX2, KIF11 and CKAP5: five specific mitosis-associated genes correlate with poor prognosis for non-small cell lung cancer patients. Int J Oncol 2017; 50: 365-372.
[65] Wang C, Yan Q, Hu M, Qin D and Feng Z. Effect of AURKA gene expression knockdown on angiogenesis and tumorigenesis of human ovarian cancer cell lines. Target Oncol 2016; 11: 771-781.
[66] Katsha A, Arras J, Soutto M, Belkhiri A and El-Rifai W. AURKA regulates JAK2-STAT3 activity in human gastric and esophageal cancers. Mol Oncol 2014; 8: 1419-1428.
[67] Lee MG and Nurse P. Complementation used to clone a human homologue of the fission yeast cell cycle control gene cdc2. Nature 1987; 327: 31-35.
[68] Willder JM, Heng SJ, McCall P, Adams CE, Tannahill C, Fyffe G, Seywright M, Horgan PG, Leung HY, Underwood MA and Edwards J. Androgen receptor phosphorylation at serine 515 by Cdk1 predicts biochemical relapse in prostate cancer patients. Br J Cancer 2013; 108: 139-148.
[69] Izadi S, Nikkhoo A, Hojjat-Farsangi M, Namdar A, Azizi G, Mohammadi H, Yousefi M and Jadidi-Niaragh F. CDK1 in breast cancer: implications for theranostic potential. Anticancer Agents Med Chem 2020; 20: 758-767.
[70] Kim S, Nakayama S, Miyoshi Y, Taguchi T, Tamaki Y, Matsushima T, Torikoshi Y, Tanaka S, Yoshida T, Ishihara H and Noguchi S. Determination of the specific activity of CDK1 and CDK2 as a novel prognostic indicator for early breast cancer. Ann Oncol 2008; 19: 68-72.
[71] Li M, He F, Zhang Z, Xiang Z and Hu D. CDK1 serves as a potential prognostic biomarker and target for lung cancer. J Int Med Res 2020; 48: 300060519897508.
[72] Shi YX, Zhu T, Zou T, Zhuo W, Chen YX, Huang MS, Zheng W, Wang CJ, Li X, Mao XY, Zhang W, Zhou HH, Yin JY and Liu ZQ. Prognostic and predictive values of CDK1 and MAD2L1 in lung adenocarcinoma. Oncotarget 2016; 7: 85235.
[73] Zheng HP, Huang ZG, He RQ, Lu HP, Dang YW, Lin P, Wen DY, Qin YY, Luo B, Li XJ, Mo WJ, Yang H, He Y and Chen G. Integrated assessment of CDK1 upregulation in thyroid cancer. Am J Transl Res 2019; 11: 7233.
[74] Luo Y, Wu Y, Peng Y, Liu X, Bie J and Li S. Systematic analysis to identify a key role of CDK1 in mediating gene interaction networks in cervical cancer development. Ir J Med Sci 2016; 185: 231-239.
[75] Chang JT, Wang HM, Chang KW, Chen WH, Wen MC, Hsu YM, Yung BYM, Chen IH, Liao CT, Hsieh LL and Cheng AJ. Identification of differentially expressed genes in oral squamous cell carcinoma (OSCC): overexpression of NPM, CDK1 and NDRG1 and underexpression of CHES1. Int J Cancer 2005; 114: 942-9.
[76] Menon DR, Luo Y, Arcaroli JJ, Liu S, Krishnan-Kutty LN, Osborne DG, Li Y, Samson JM, Bagby S, Tan AC, Robinson WA, Messersmith WA and Fujita M. CDK1 interacts with Sox2 and promotes tumor initiation in human melanoma. Cancer Res 2018; 78: 6561-6574.
[77] Huang J, Chen P, Liu K, Liu J, Zhou B, Wu R, Peng Q, Liu ZX, Li C, Kroemer G, Lotze M, Zeh H, Kang R and Tang D. CDK1/2/5 inhibition overcomes IFNG-mediated adaptive immune resistance in pancreatic cancer. Gut 2021; 70: 890-899.
[78] Bae T, Weon KY, Lee JW, Eum KH, Kim S and Choi JW. Restoration of paclitaxel resistance by CDK1 intervention in drug-resistant ovarian cancer. Carcinogenesis 2015; 36: 1561-1571.
[79] Zhang R, Shi H, Ren F, Zhang M, Ji P, Wang W and Liu C. The aberrant upstream pathway regulations of CDK1 protein were implicated in the proliferation and apoptosis of ovarian cancer cells. J Ovarian Res 2017; 10: 1-11.
[80] Seeruttun SR, Cheung WY, Wang W, Fang C, Liu ZM, Li JQ, Wu T, Wang J, Liang C and Zhou ZW. Identification of molecular biomarkers for the diagnosis of gastric cancer and lymph-node metastasis. Gastroenterol Rep 2018; 7: 57-66.
[81] Tagami H, Ray-Gallet D, Almouzni G and Nakatani Y. Histone H3. 1 and H3. 3 complexes mediate nucleosome assembly pathways dependent or independent of DNA synthesis. Cell 2004; 116: 51-61.
[82] Mello JA, Silljé HH, Roche DM, Kirschner DB, Nigg EA and Almouzni G. Human Asf1 and CAF-1 interact and synergize in a repair-coupled nucleosome assembly pathway. EMBO Rep 2002; 3: 329-334.
[83] Han G, Zhang X, Liu P, Yu Q, Li Z, Yu Q and Wei X. Knockdown of anti-silencing function 1B histone chaperone induces cell apoptosis via repressing PI3K/Akt pathway in prostate cancer. Int J Oncol 2018; 53: 2056-2066.
[84] Corpet A, De Koning L, Toedling J, Savignoni A, Berger F, Lemaître C, O'sullivan RJ, Karlseder J, Barillot E and Asselain B. Asf1b, the necessary Asf1 isoform for proliferation, is predictive of outcome in breast cancer. EMBO J 2011; 30: 480-493.
[85] Liang X, Yuan X, Yu J, Wu Y, Li K, Sun C, Li S, Shen L, Kong F and Jia J. Histone chaperone ASF1A predicts poor outcomes for patients with gastrointestinal cancer and drives cancer progression by stimulating transcription of β-catenin target genes. EBioMedicine 2017; 21: 104-116.

[86] Jiangqiao Z, Tao Q, Zhongbao C, Xiaoxiong M, Long Z, Jilin Z and Tianyu W. Anti-silencing function 1B histone chaperone promotes cell proliferation and migration via activation of the AKT pathway in clear cell renal cell carcinoma. Biochem Biophys Res Commun 2019; 511: 165-172.
[87] Chen Z, Ou D, Huang Z and Shen P. Identification of hsa_circ_0002024 as a prognostic competing endogenous RNA (ceRNA) through the hsa_miR_129-5p/Anti-Silencing Function 1B histone chaperone (ASF1B) axis in renal cell carcinoma. Bioengineered 2021; 12: 6579-6593.
[88] Zhang W, Gao Z, Guan M, Liu N, Meng F and Wang G. ASF1B promotes oncogenesis in lung adenocarcinoma and other cancer types. Front Oncol 2021; 11: 36-48.
[89] Zhang W, Li H, Sun X, Shi Y, Yang Y, Xie C and Yanna Z. Anti-silencing function 1B overexpression affects prognosis and promotes invasion in cervical carcinoma via activation of Wnt/β-catenin signaling pathway. 2021.
[90] Jacobsen A, Bosch LJW, Martens-de Kemp SR, Carvalho B, Sillars-Hardebol AH, Dobson RJ, de Rinaldis E, Meijer GA, Abeln S, Heringa J, Fijneman RJA and Feenstra KA. Aurora kinase A (AURKA) interaction with Wnt and Ras-MAPK signalling pathways in colorectal cancer. Sci Rep 2018; 8: 7522.
[91] Hu X, Zhu H, Zhang X, He X and Xu X. Comprehensive analysis of pan-cancer reveals potential of ASF1B as a prognostic and immunological biomarker. Cancer Med 2021; 19: 6897-6916.
[92] Li M, Huang L, Xiao Y, Wang C, Li Q and Qin C. Elevated ASF1B promotes apoptosis in gastric tumour cells through the Bax/Bcl-2-p53 pathway and is related to a good prognosis. 2021.
[93] Lenormand JL, Dellinger RW, Knudsen KE, Subramani S and Donoghue DJ. Speedy: a novel cell cycle regulator of the G2/M transition. EMBO J 1999; 18: 1869-1877.
[94] Pandey JP, Namboodiri AM and Kistner-Griffin E. A genetic variant of FcγRIIIa is strongly associatedwith humoral immunity to cyclin B1 in African American patients with prostate cancer. Immunogenetics 2013; 65: 91-96.
[95] Wang A, Yoshimi N, Ino N, Tanaka T and Mori H. Overexpression of cyclin B1 in human colorectal cancers. J Cancer Res Clin Oncol 1997; 123: 124-127.
[96] Kushner J, Bradley G, Young B and Jordan RC. Aberrant expression of cyclin A and cyclin B1 proteins in oral carcinoma. J Oral Pathol Med 1999; 28: 77-81.
[97] Yang WX, Pan YY and You CG. CDK1, CCNB1, CDC20, BUB1, MAD2L1, MCM3, BUB1B, MCM2, and RFC4 may be potential therapeutic targets for hepatocellular carcinoma using integrated bioinformatic analysis. Biomed Res Int 2019; 13; 1245072.
[98] Chen EB, Qin X, Peng K, Li Q, Tang C, Wei YC, Yu S, Gan L and Liu TS. HnRNPR-CCNB1/CENPF axis contributes to gastric cancer proliferation and metastasis. Aging 2019; 11: 7473.
[99] Nozoe T, Korenaga D, Kabashima A, Ohga T, Saeki H and Sugimachi K. Significance of cyclin B1 expression as an independent prognostic indicator of patients with squamous cell carcinoma of the esophagus. Clin Cancer Res 2002; 8: 817-22.
[100] Wang F, Chen X, Yu X and Lin Q. Degradation of CCNB1 mediated by APC11 through UBA52 ubiquitination promotes cell cycle progression and proliferation of non-small cell lung cancer cells. Am J Transl Res 2019; 11: 7166.
[101] Arora S, Singh P, Rahmani AH, Almatroodi SA, Dohare R and Syed MA. Unravelling the role of miR-20b-5p, CCNB1, HMGA2 and E2F7 in development and progression of non-small cell lung cancer (NSCLC). Biology (Basel) 2020; 9: 201.
[102] Zhang H, Zhang X, Li X, Meng WB, Bai ZT, Rui SZ, Wang ZF, Zhou WC and Jin XD. Effect of CCNB1 silencing on cell cycle, senescence, and apoptosis through the p53 signaling pathway in pancreatic cancer. J Cell Physiol 2019; 234: 619-631.
[103] Li S, Liu N, Piao J, Meng F and Li Y. CCNB1 expedites the progression of cervical squamous cell carcinoma via the regulation by FOXM1. Onco Targets Ther 2020; 13: 12383.
[104] Li Q, Zhang L, Jiang J, Zhang Y, Wang X, Zhang Q, Wang Y, Liu C and Li F. CDK1 and CCNB1 as potential diagnostic markers of rhabdomyosarcoma: validation following bioinformatics analysis. BMC Med Genomics 2019; 12: 1-13.
[105] Xia A, Zhang Y, Xu J, Yin T and Lu XJ. T cell dysfunction in cancer immunity and immunotherapy. Front Immunol 2019; 10: 1719-1719.
[106] Jiang T, Shi J, Dong Z, Hou L, Zhao C, Li X, Mao B, Zhu W, Guo X and Zhang H. Genomic landscape and its correlations with tumor mutational burden, PD-L1 expression, and immune cells infiltration in Chinese lung squamous cell carcinoma. J Hematol Oncol 2019; 12: 1-13.
[107] Trojan A, Urosevic M, Dummer R, Giger R, Weder W and Stahel RA. Immune activation status of CD8+ T cells infiltrating non-small cell lung cancer. Lung Cancer 2004; 44: 143-147.
[108] Kelsey R. NRG1 can promote antiandrogen resistance. Nat Rev Urol 2020; 17: 486.
[109] Song ZY, Chao F, Zhuo Z, Ma Z, Li W and Chen G. Identification of hub genes in prostate cancer using robust rank aggregation and weighted gene co-expression network analysis. Aging 2019; 11: 4736-4756.

[110] Fang E, Zhang X, Wang Q and Wang D. Identification of prostate cancer hub genes and therapeutic agents using bioinformatics approach. Cancer Biomark 2017; 20: 553-561.
[111] Ye Y, Li SL and Wang SY. Construction and analysis of mRNA, miRNA, lncRNA, and TF regulatory networks reveal the key genes associated with prostate cancer. PLoS One 2018; 13: e0198055.
[112] Shao N, Yuan K, Zhang Y, Yun Cheang T, Li J and Lin Y. Identification of key candidate genes, pathways and related prognostic values in ER-negative/HER2-negative breast cancer by bioinformatics analysis. J BUON 2018; 23: 891-901.
[113] Lu W and Ding Z. Identification of key genes in prostate cancer gene expression profile by bioinformatics. Andrologia 2019; 51: e13169.
[114] Pashaei E, Pashaei E, Ahmady M, Ozen M and Aydin N. Meta-analysis of miRNA expression profiles for prostate cancer recurrence following radical prostatectomy. PLoS One 2017; 12: e0179543.
[115] Xu N, Wu YP, Ke ZB, Liang YC, Cai H, Su WT, Tao X, Chen SH, Zheng QS, Wei Y and Xue XY. Identification of key DNA methylation-driven genes in prostate adenocarcinoma: an integrative analysis of TCGA methylation data. J Transl Med 2019; 17: 311.
[116] Wang Y, Xu H, Zhu B, Qiu Z and Lin Z. Systematic identification of the key candidate genes in breast cancer stroma. Cell Mol Biol Lett 2018; 23: 44.
[117] Huang H, Zhang Q, Ye C, Lv JM, Liu X, Chen L, Wu H, Yin L, Cui XG and Xu DF. Identification of prognostic markers of high grade prostate cancer through an integrated bioinformatics approach. J Cancer Res Clin Oncol 2017; 143: 2571-2579.
[118] Yin X, Yu J, Zhou Y, Wang C, Jiao Z, Qian Z, Sun H and Chen B. Identification of CDK2 as a novel target in treatment of prostate cancer. Future Oncol 2018; 14: 709-718.
[119] Foj L and Filella X. Identification of potential miRNAs biomarkers for high-grade prostate cancer by integrated bioinformatics analysis. Pathol Oncol Res 2019; 25: 1445-1456.
[120] Chen J, Liu C, Cen J, Liang T, Xue J, Zeng H, Zhang Z, Xu G, Yu C, Lu Z, Wang Z, Jiang J, Zhan X and Zeng J. KEGG-expressed genes and pathways in triple negative breast cancer: protocol for a systematic review and data mining. Medicine 2020; 99: e19986.
[121] Lin Y, Fu F, Lv J, Wang M, Li Y, Zhang J and Wang C. Identification of potential key genes for HER-2 positive breast cancer based on bioinformatics analysis. Medicine 2020; 99: e18445.
[122] Li S, Hou J and Xu W. Screening and identification of key biomarkers in prostate cancer using bioinformatics. Mol Med Rep 2020; 21: 311-319.
[123] Guo L, Lin M, Cheng Z, Chen Y, Huang Y and Xu K. Identification of key genes and multiple molecular pathways of metastatic process in prostate cancer. PeerJ 2019; 7: e7899.
[124] Wu YP, Ke ZB, Lin F, Wen YA, Chen S, Li XD, Chen SH, Sun XL, Huang JB, Zheng QS, Xue XY, Wei Y and Xu N. Identification of key genes and pathways in castrate-resistant prostate cancer by integrated bioinformatics analysis. Pathol Res Pract 2020; 216: 153109.
[125] He Z, Duan X and Zeng G. Identification of potential biomarkers and pivotal biological pathways for prostate cancer using bioinformatics analysis methods. PeerJ 2019; 7: e7872.
[126] Zheng L, Dou X, Ma X and Qu W. Identification of potential key genes and pathways in enzalutamide-resistant prostate cancer cell lines: a bioinformatics analysis with data from the Gene Expression Omnibus (GEO) database. Biomed Res Int 2020; 2020: 8341097.

References

[1] Song ZY, Chao F, Zhuo Z, Ma Z, Li W and Chen G. Identification of hub genes in prostate cancer using robust rank aggregation and weighted gene co-expression network analysis. Aging 2019; 11: 4736-4756.

[2] Fang E, Zhang X, Wang Q and Wang D. Identification of prostate cancer hub genes and therapeutic agents using bioinformatics approach. Cancer Biomark 2017; 20: 553-561.

[3] Ye Y, Li SL and Wang SY. Construction and analysis of mRNA, miRNA, lncRNA, and TF regulatory networks reveal the key genes associated with prostate cancer. PLoS One 2018; 13: e0198055.

[4] Shao N, Yuan K, Zhang Y, Yun Cheang T, Li J and Lin Y. Identification of key candidate genes, pathways and related prognostic values in ER-negative/HER2-negative breast cancer by bioinformatics analysis. J BUON 2018; 23: 891-901.

[5] Lu W and Ding Z. Identification of key genes in prostate cancer gene expression profile by bioinformatics. Andrologia 2019; 51: e13169.

[6] Xu N, Wu YP, Ke ZB, Liang YC, Cai H, Su WT, Tao X, Chen SH, Zheng QS, Wei Y and Xue XY. Identification of key DNA methylation-driven genes in prostate adenocarcinoma: an integrative analysis of TCGA methylation data. J Transl Med 2019; 17: 311.

[7] Wang Y, Xu H, Zhu B, Qiu Z and Lin Z. Systematic identification of the key candidate genes in breast cancer stroma. Cell Mol Biol Lett 2018; 23: 44.

[8] Huang H, Zhang Q, Ye C, Lv JM, Liu X, Chen L, Wu H, Yin L, Cui XG and Xu DF. Identification of prognostic markers of high grade prostate cancer through an integrated bioinformatics approach. J Cancer Res Clin Oncol 2017; 143: 2571-2579.

[9] Yin X, Yu J, Zhou Y, Wang C, Jiao Z, Qian Z, Sun H and Chen B. Identification of CDK2 as a novel target in treatment of prostate cancer. Future Oncol 2018; 14: 709-718.

[10] Foj L and Filella X. Identification of potential miRNAs biomarkers for high-grade prostate cancer by integrated bioinformatics analysis. Pathol Oncol Res 2019; 25: 1445-1456.

[11] Chen J, Liu C, Cen J, Liang T, Xue J, Zeng H, Zhang Z, Xu G, Yu C, Lu Z, Wang Z, Jiang J, Zhan X and Zeng J. KEGG-expressed genes and pathways in triple negative breast cancer: protocol for a systematic review and data mining. Medicine 2020; 99: e19986.

[12] Lin Y, Fu F, Lv J, Wang M, Li Y, Zhang J and Wang C. Identification of potential key genes for HER-2 positive breast cancer based on bioinformatics analysis. Medicine 2020; 99: e18445.

[13] Li S, Hou J and Xu W. Screening and identification of key biomarkers in prostate cancer using bioinformatics. Mol Med Rep 2020; 21: 311-319.

[14] Guo L, Lin M, Cheng Z, Chen Y, Huang Y and Xu K. Identification of key genes and multiple molecular pathways of metastatic process in prostate cancer. PeerJ 2019; 7: e7899.

[15] Wu YP, Ke ZB, Lin F, Wen YA, Chen S, Li XD, Chen SH, Sun XL, Huang JB, Zheng QS, Xue XY, Wei Y and Xu N. Identification of key genes and pathways in castrate-resistant prostate cancer by integrated bioinformatics analysis. Pathol Res Pract 2020; 216: 153109.

[16] He Z, Duan X and Zeng G. Identification of potential biomarkers and pivotal biological pathways for prostate cancer using bioinformatics analysis methods. PeerJ 2019; 7: e7872.

[17] Zheng L, Dou X, Ma X and Qu W. Identification of potential key genes and pathways in enzalutamide-resistant prostate cancer cell lines: a bioinformatics analysis with data from the Gene Expression Omnibus (GEO) database. Biomed Res Int 2020; 2020: 8341097.

Supplementary Table 1. Row list of PRAD-associated hub genes extracted from previous studies

Dataset	Name of hub genes	No. of hub genes	Reference
GSE6919 GSE6956 GSE32448 GSE32571 GSE35988 GSE46602 GSE68555 GSE69223 GSE70768 GSE88808	RRM2, KIFC1, TACC3, PRC1, BIRC5, CDK1, ASF1B, E2F1, RACGAP1, MYBL2, TPX2, CDC20, TOP2A, NUSAP1, UBE2T, LMNB1, CCNB1, ZWINT, STMN1, and TK1	20	[1]
GSE26910	CDH1, BMP2, NKX3-1, PPARG and PRKAR2B	6	[2]
GSE64318 GSE46602	EGFR, VEGFA, PIK3R1, DLG4, TGFBR1 and KIT	6	[3]
GSE55945 GSE60329 GSE103512	HSPA8, PPP2R1A, CTNNB1, ADCY5, ANXA1, and COL9A2	6	[4]
GSE32448 GSE45016 GSE46602 GSE104749	EPCAM, TWIST1, CD38 and VEGFA	6	[5]
GSE55323 GSE26245 GSE26247 GSE65061 GSE62610 GSE46738	TCF3, MYC, MAX, CYP26A1 and SREBF1	5	[6]
GSE112047 GSE76938	IFITM1, RTP4, ACSF2, GSTM2, GSTM1, ACOX2, COL4A6, ITGA2, AKR1B1, NPY, CFTR, GPX7, ALDH3A1, CRYZ, ALDH2, MAOB, GSTP1, GPX3, XAF1, and BST2	19	[7]
GSE7930	FABP4, IGFBP3, THBS1, and GJA1	4	[8]
GSE32571	UBE2C, KIF20A, CDC20, PTTG1 and TOP2A	5	[9]
GSE6605 GSE6606	TPM1, TAGLN, LMOD1, MYLK, ACTA2, TPM2, ACTG2, MYH11, MYL9 and CALD1	10	[10]
GSE26022 GSE30521 GSE46602	EGFR, VEGFA, IGF1, PIK3R1, CD44, ITGB4, ANXA1, BCL2, LPAR3, LPAR1	10	[11]
GSE69223	CCNB1, TTK, CNN1, and ACTG2	4	[12]
GSE3325 GSE6919	PBK, RAP1A, GNAS, RAB39B, COPZ2, KLF4, BACE1 and COL12A1	8	[13]
GSE70768	ALB, ACACB, KLK3, CDH1, IL10, ALDH1A3, KLK2, ALDH3B2, HBA1, COL1A1	10	[14]
GSE104935 GSE64143 GSE120005	NMU, GAL, LPAR3, F2RL1, PTGFR, AR, CXCR7, CCR7, NDRG1, NK3, NKX3-1	11	[15]
GSE6919 GSE32269	UBE2C, CCNB2, CKS2, HMMR, AR, CDKN3, TPX2, AURKA, SPP1, FOS	10	[16]
GSE103512	KLK3, CDH1, KLK2, FOXA1, EPCAM	5	[17]

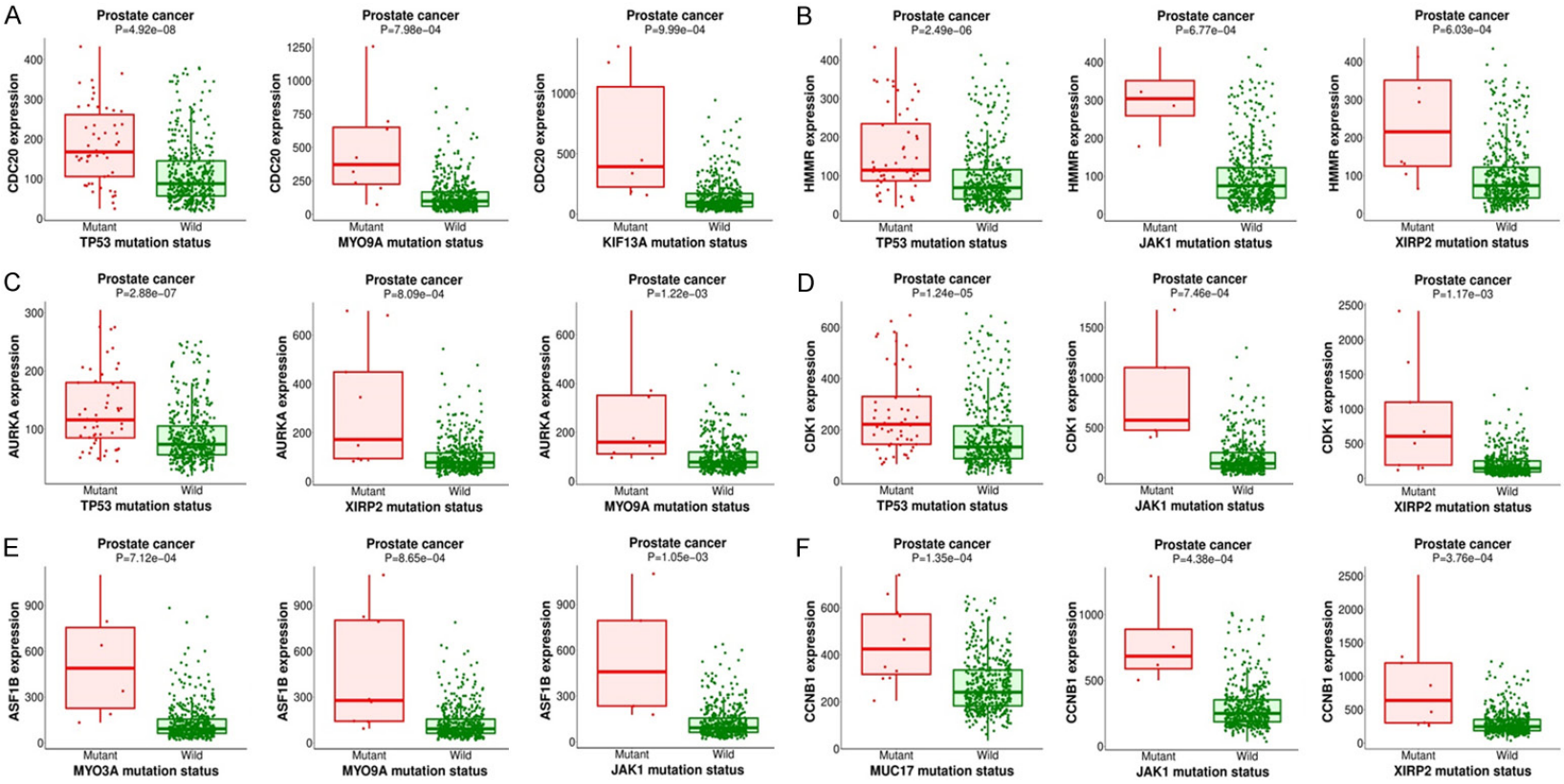

Supplementary Figure 1. Real hub genes positively correlated with mutant genes in PRAD from MuTarget. (A) Top 3 correlated genes with CDC20, (B) Top 3 correlated genes with HMMR, (C) Top 3 correlated genes with AURKA, (D) Top 3 correlated genes with CDK1, (E) Top 3 correlated genes with ASF1B, and (F) Top 3 correlated genes with CCNB1. A *p*-value <0.05 was significant.

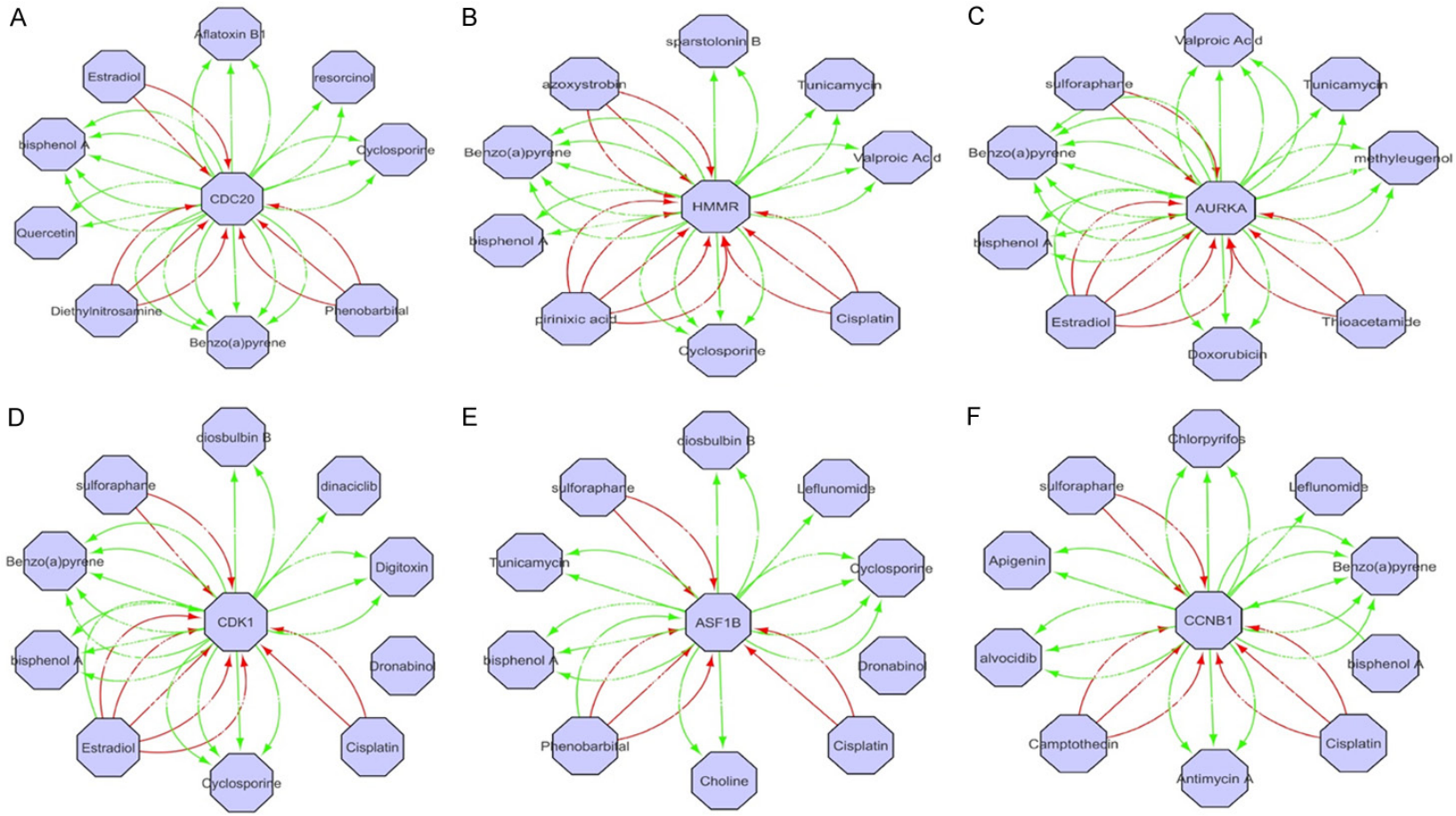

Supplementary Figure 2. Screening of real hub genes associated with chemotherapeutic drugs. (A-F) Indicates chemotherapeutic drugs that can decrease or increase the expression of the real hub genes. (A) CDC20 relevant drugs, (B) HMMR relevant drugs, (C) AURKA relevant drugs, (D) CDK1 relevant drugs, (E) ASF1B relevant drugs, and (F) CCNB1 relevant drugs. Red arrows: drugs that increase expression, Green arrows: drug that decrease expression. The numbers of arrows represent the number of supportive studies in the literature.